



## Heat exchangers for hydrogen tank filling

| IFE/E-2023/002 |

Research for a better future

Report number: <b>IFE/E-2023/002</b>	ISSN: 2535-6380	Availability: Public	Report date: 20-01-2023
Revision:	ISBN: <b>978-82-7017-940-4</b>	DOCUS-ID: 57582	Number of pages: 33
Client: H2Maritime project			
Title: <b>Heat exchangers for hydrogen tank filling</b>			
Summary:  The purpose of this report is to give some basic facts about heat exchangers and summarize a series of simulations done on counter-flow concentric tube heat exchangers for hydrogen gas bunkering using the COMSOL Multiphysics software. Part 1 of this report consists of an exploration of how various system parameters (flowrates, pressures, and tube dimensions) influence the properties of a heat exchangers based on pure water as coolant. Part 2 discusses how the heat exchanger performance can be improved using ethylene glycol-water mixtures and compares these results to those using pure water coolant. The Appendix gives tables of heat transfer coefficients for heat exchangers of different sizes using pure water and ethylene glycol-water mixtures.			
Prepared by:	Geir Helgesen	DocuSigned by:  4D3ECF7FFB2C42B...	
Reviewed by:	Øystein Ulleberg	DocuSigned by: 	
Approved by:	Ragnhild Hancke	0100F9BD237F4F... DocuSigned by: 	
Report distribution:	A0DE7A050B5C4EA...		

Report – H2Maritime project  
Heat exchangers for hydrogen tank filling

Geir Helgesen

January 20, 2023

Institute for Energy Technology  
Department for hydrogen technology  
NO-2027 Kjeller, Norway

## Contents

1	Introduction	5
2	Heat exchangers	5
2.1	Theory of counter-flow systems . . . . .	6
3	Simulation of heat exchangers	7
3.1	Basic description . . . . .	7
3.2	Simulation on a HX system of fixed size . . . . .	8
3.3	Exploring effects of HX tube sizes . . . . .	11
4	Discussion - using water as coolant	12
5	Conclusion of Part 1	13
6	Cooling using other water-based refrigerants	14
7	Comparisons of efficiency of water and EG-water as coolant	15
8	Coolant flow patterns and cooling capacity	19
8.1	Flow velocity and pressure drops . . . . .	19
8.2	Velocity and temperature distributions . . . . .	19
9	Temperature estimates based on heat transfer coefficients	21
10	Summary and Conclusion of Part 2	23
A	Appendix - Calculation of heat transfer coefficients	26
B	Appendix - EES software for temperature calculation of hydrogen tank bunkering process	31

## List of symbols

$A_s$	.....	surface area of heat exchanger
$c_p$	.....	heat capacity
$C_r$	.....	capacity ratio
$h$	.....	heat convection coefficient of fluid
$k$	.....	thermal conductivity of tube metal wall
$L$	.....	tube length
LMTD, $\Delta T_{lm}$	.....	log-mean temperature difference
$\dot{m}_h, \dot{m}_{H_2}$	.....	mass flowrate of hot fluid or hydrogen gas (unit kg/s)
$\dot{m}_c, \dot{m}_{H_2O}$	.....	mass flowrate of cold fluid, coolant or water (unit kg/s)
NTU	.....	number of transfer units
$P_{in}, P_{out}$	.....	inlet and outlet gas pressures
$Pr$	.....	Prandtl number
$\dot{Q}$	.....	cooling power, heat transfer rate (unit kW)
$R$	.....	thermal resistance
$r_i, r_o$	.....	inner and outer tube radius
$Re$	.....	Reynolds number
$T_{h,in}, T_{h,out}, T_{c,in}, T_{c,out}$	.....	inlet and outlet temperatures of hot and cold fluids
$U$	.....	effective heat transfer coefficient (unit $W/m^2 \cdot K$ )
$v_g, v_{cool}$	.....	velocity of gas and coolant (unit m/s)
$\varepsilon$	.....	effectiveness
$\eta$	.....	viscosity of fluid
$\rho$	.....	density of fluid
$\kappa$	.....	thermal conductivity of fluid
$\mu_{JT}$	.....	Joule-Thomson coefficient

## **Abstract**

The purpose of this report is to give some basic facts about heat exchangers and summarize a series of simulations done on counter-flow concentric tube heat exchangers for hydrogen gas bunkering using the COMSOL Multiphysics software. Part 1 of this report consists of an exploration of how various system parameters (flowrates, pressures and tube dimensions) influence the properties of a heat exchangers based on pure water as coolant. Part 2 discusses how the heat exchanger performance can be improved using ethylene glycol-water mixtures and compares these results to those using pure water coolant. The Appendix gives tables of heat transfer coefficients for heat exchangers of different sizes using pure water and ethylene glycol-water mixtures.

# Part 1 Water based cooling

## 1 Introduction

Hydrogen in gas or liquid form is considered to be one of the most important energy carriers of the future. However, the heat management during maritime bunkering has some challenges. The competence building project H2Maritime [1] explores future uses of hydrogen in the maritime sector, including the use of compressed H<sub>2</sub>-gas in combination with fuel cells for powering the electrical propulsion system in boats and ferries.

Almost all ordinary gases will cool down when they expand from a high pressure state ( $P_{high}, T$ ) to a lower pressure state ( $P_{low}, T$ ) for temperatures  $T$  in a range near room temperature  $25\text{ }^\circ\text{C} = 298\text{ K}$ . However, both hydrogen and helium gas have the peculiar property that they will heat up when the gas expands near ambient temperatures when there is no or very limited heat transfer from the surroundings, i.e., adiabatic expansion (isenthalpic - constant enthalpy  $H$ ) or during fast filling. This can be quantified by observing that their Joule-Thomson coefficient  $\mu_{JT} = \left(\frac{\partial T}{\partial P}\right)_H$  is negative, which occurs for all temperatures above  $T_i \approx 200\text{ K}$  (called the inversion temperature).[2] This leads to a significant heating when pressurized hydrogen tanks are filled from a higher pressure reservoir. Typically, the pressure in such tanks can be in the range 300 - 700 bar. Near room temperature and at pressure 600 bar,  $\mu_{JT} = -0.05\text{ K/bar}$  and decreases slightly at lower pressures.

For light-weight tanks based on composite materials with polymer linings on the inside, this causes problems since such linings typically can be damaged by heating above about  $75 - 85\text{ }^\circ\text{C}$  [3]. Melting point of some of the liners can be as low as  $120\text{ }^\circ\text{C}$ . Ideally, a tank containing about 1 ton (1000 kg) should preferentially be filled up from nearly empty state in less than one half hour, which will lead to a compressed gas mass transfer rate  $\dot{m}_{H_2}$  more than 0.5 kg/s. Heat transfer modeling based on the Engineering Equation Solver software (EES) [4] indicates that a cooling power of  $\dot{Q} \approx 500 - 1000\text{ kW}$  will be needed in the initial phases of tank filling in order to keep the temperature inside the tank below about  $75\text{ }^\circ\text{C}$ . How can such cooling rates be obtained in practice?

The simplest would be to use heat exchangers based on a cold water (or another cold liquid) flowing around the gas inlet pipe to the tank. In the simulations presented below some results from finite element, mathematical heat transfer modeling of heat exchangers will be presented.

## 2 Heat exchangers

Heat exchangers (HX) come in a variety of different types [5, 6, 7]. The simplest are double pipe heat exchangers where one fluid is flowing in a tube mounted inside an outer tube containing another fluid (liquid or gas) - the coolant - in the “annulus region”. These come in two main types, *parallel flow* with both fluids entering on the same side and *counter flow* where the flow direction of the fluids are opposite. Such double pipe exchangers can also be made into more complex, bent shapes (e.g. *multi-pass HX*), and fins can be added to increase the effective surfaces area between the two fluids.

In other types of heat exchangers, the flow directions of the fluid are perpendicular to

each other, so-called *cross-flow HX*. Also, larger shell-and-tube heat exchangers, with a large number of tubes packed into an outer shell, are used in industrial applications. Larger temperature changes in one of the fluids can be obtained by using condensers or evaporators. In these, one of the fluids transfer or absorb heat from the other fluid by changing from gas to liquid state (or the opposite).

## 2.1 Theory of counter-flow systems

In double pipe heat exchangers the thermal resistance  $R$  to heat transfer from hot fluid to the colder fluid can be modeled similar to a resistor network

$$R_{total} = R_{inner} + R_{wall} + R_{outer} = \frac{1}{h_i 2\pi r_i} + \frac{\ln(r_o/r_i)}{2\pi k L} + \frac{1}{h_o 2\pi r_o} \equiv \frac{1}{U \cdot A_s}, \quad (1)$$

where  $h_i, h_o$  and  $k$  are the *heat convection coefficients* of the fluids, and thermal conductivity of the tube metal, respectively.  $r_i$  and  $r_o$  are radius of the inner and outer tubes, and  $L$  is the length of the tubes.  $U$  is the *effective heat transfer coefficient* and  $A_s$  is the effective heat transfer surface. The effective heat transfer coefficient in units of  $W/m^2 \cdot K$  vary from 10-40 for gas-to-gas systems to 1000 or more for liquid-liquid systems (e.g. water-to-water) and can reach up to 10000 for evaporators and condensers. The product  $U A_s$  (in  $W/K$ ) is the important parameter for characterizing a heat exchanger system.

The heat transfer will be dominated by the smallest heat transfer coefficient of the fluids if they are significantly different. In many cases the thermal resistance in the wall  $R_{wall}$  can be neglected (i.e. thin wall) and if  $h_1 \ll h_2$  (1 or 2 being inner or outer), then  $U \approx h_1$ . This can often occur when one fluid is a gas and the other is a liquid.

In order to characterize heat exchangers, various characteristic numbers are used. To have *one* typical number for the temperature difference between the two sides the *Log-Mean Temperature Difference* (LMTD) is often used. LMTD can be defined as

$$\Delta T_{lm} = \frac{\Delta T_1 - \Delta T_2}{\ln(\Delta T_1/\Delta T_2)}, \quad (2)$$

and the *effective heat transfer rate* can be calculated as

$$\dot{Q} = U A_s \Delta T_{lm}. \quad (3)$$

The definitions of the temperature differences  $\Delta T_1$  and  $\Delta T_2$  depend on the type of double pipe HX. Using  $h$  and  $c$  for hot and cold flow, then for parallel flow HX  $\Delta T_1 = T_{h,in} - T_{c,in}$  and  $\Delta T_2 = T_{h,out} - T_{c,out}$ . For counter-flow they are  $\Delta T_1 = T_{h,in} - T_{c,out}$  and  $\Delta T_2 = T_{h,out} - T_{c,in}$ . This corresponds to the temperature differences between the fluids at the two ends of the HX pipes. It can be shown that LMTD for a counter-flow heat exchanger will always be larger than that for a similar parallel flow HX, and thus will be more energy efficient. For more complex types of heat exchangers a correction factor for the shape has to be taken into the definition of LMTD.

The effectiveness  $\varepsilon$  of a heat exchanger depends on its geometry and on the flow arrangement. With  $\dot{m}_c$  and  $\dot{m}_h$  being the mass flowrate (in kg/s) of the cold and hot fluids and  $c_p$



being their heat capacities and assuming  $\dot{m}_c c_{p,c} > \dot{m}_h c_{p,h}$ , this parameter is defined as

$$\varepsilon = \frac{\dot{Q}}{\dot{Q}_{max}} = \frac{T_{h,in} - T_{h,out}}{T_{h,in} - T_{c,in}}. \quad (4)$$

If  $\dot{m}_c c_{p,c} < \dot{m}_h c_{p,h}$ , then  $T_{h,in} - T_{h,out}$  is replaced by  $T_{c,out} - T_{c,in}$  in the equation above.

Sometimes it may be convenient to calculate the effectiveness of a HX from dimensionless numbers. This can be done by introducing the dimensionless number called *Number of Transfer Units NTU* defined as

$$NTU = \frac{UA_s}{(\dot{m}c_p)_{min}}, \quad (5)$$

where subscript *min* refers to the smallest of the values for the hot and the cold fluids. Also, one defines the *capacity ratio*  $C_r$  as

$$C_r = \frac{(\dot{m}c_p)_{min}}{(\dot{m}c_p)_{max}}. \quad (6)$$

The effectiveness can then be written as a function of  $NTU$  and  $C_r$ ,  $\varepsilon = \varepsilon(NTU, C_r)$ . For counter-flow HX, the relationship between  $NTU$  and  $\varepsilon$  is

$$NTU = \frac{1}{C_r - 1} \ln \left( \frac{\varepsilon - 1}{\varepsilon C_r - 1} \right). \quad (7)$$

Effectiveness  $\varepsilon$  as a function of  $NTU$  and  $C_r$  for various types of heat exchangers can be found in tables, with values ranging between 0 and 1. The  $\varepsilon$ -value increases strongly with  $NTU$  for  $NTU < 1.5$  and then levels off (see Fig. 1b). For fixed value of  $NTU$ ,  $\varepsilon$  increases with decreasing  $C_r$ , most clearly for  $NTU > 2$ . However, this  $C_r$ -dependence is smallest for counter-flow heat exchangers.

### 3 Simulation of heat exchangers

#### 3.1 Basic description

Heat transfer rate  $\dot{Q}$  and effectiveness  $\varepsilon$  for heat exchangers can be estimated based on tabulated values. However, in order to get more realistic and detailed information on how a heat exchanger will perform in hydrogen tank filling applications, detailed computer simulations can be done based on the thermodynamic laws and finite element computer simulations meth-

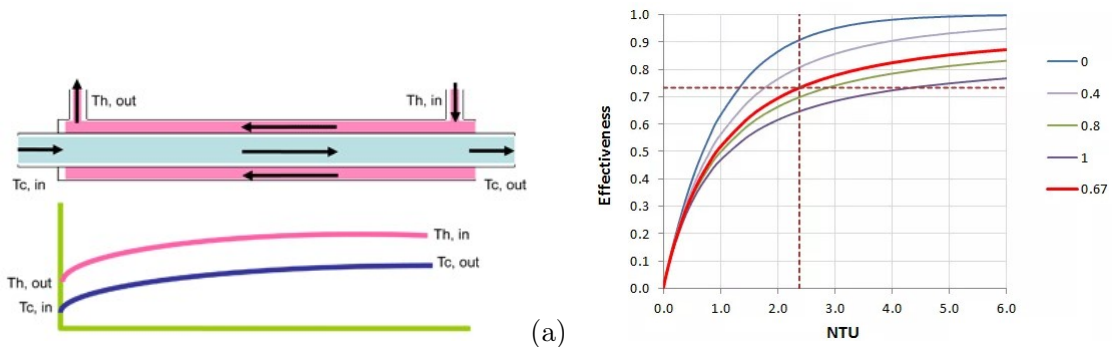


Figure 1: a) Counter-flow heat exchanger and b) effectiveness  $\varepsilon$  as function of  $NTU$  and  $C_r$ . The colors are for different values of  $C_r$ .

ods. The specific values of  $UA_s$  can be obtained under various design and flow conditions. In the current project the commercial software package COMSOL Multiphysics [8] was used to build a model of a counter-flow heat exchanger and calculate values of temperature drop and heat transfer rate in the  $H_2$  gas based on the temperature and mass flow rate of the gas.

The basic model consisted of two concentric tubes of structural steel with 1 mm wall thickness. In the initial modeling the radius of the inner tube was  $r_i = 25$  mm and of the outer  $R = r_o = 40$  mm, and the length of this tube HX, which was assumed to be straight, was  $L = 10$  m. This corresponds to an effective heat transfer surface of  $A_s = 1.57$  m<sup>2</sup>. Based on earlier model calculations for filling of larger gas tanks of size 30 – 50 m<sup>3</sup> containing about 1000 kg of gas in less than one hour, hydrogen mass flow rates in the the range  $0.5 \text{ kg/s} \leq \dot{m}_{H_2} \leq 1 \text{ kg/s}$  will be needed. For a simple HX system, the easiest would be to use cold water at  $T_c = 274 \text{ K} = 1^\circ \text{C}$  as the coolant. In the second part of this report the effect of changing to other types of coolant will be investigated. In the initial simulations two different values of temperature for the hot incoming  $H_2$ -gas were used, either  $T_{H_2} = T_h = 298 \text{ K} = 25^\circ \text{C}$  or  $318 \text{ K} = 45^\circ \text{C}$ .

In the simulations the exit pressure of the gas on the hydrogen side was assumed fixed at a constant pressure  $P_{out}$ , and the inlet pressure  $P_{in}$  and pressure drop  $\Delta P = P_{in} - P_{out}$  were found as results of the simulations. Their values depended on the mass flowrate  $\dot{m}_{H_2}$  of hydrogen and the temperature drop  $\Delta T = T_{in} - T_{out}$ .

In the first set of simulations, a relatively low gas exit pressure of the HX  $P_{out} = 10$  bar was assumed, corresponding to the initial filling of a nearly empty hydrogen tank. In the current model and using  $\dot{m}_{H_2} = 1 \text{ kg/s}$ , the gas inlet and outlet velocities were between  $v_g = 500$  m/s and 600 m/s. However, for  $\dot{m}_{H_2} = 1.5 \text{ kg/s}$  the outlet velocity was more than 900 m/s, which is much more than half of the speed of sound  $c$  in hydrogen at this pressure ( $c_{H_2} \approx 1365$  m/s). Therefore, it seems reasonable at this point to limit the mass flow to  $\dot{m}_{H_2} \leq 1 \text{ kg/s}$ . The pressure drops were  $\Delta P = 0.8$  bar and 3.0 bar at mass flow rates  $\dot{m}_{H_2} = 0.5 \text{ kg/s}$  and 1 kg/s, respectively.

### 3.2 Simulation on a HX system of fixed size

Figure 3a) shows the heat exchange power  $\dot{Q}$  of the system for various values of the cooling water flow rate  $\dot{m}_c$ , gas inlet temperatures  $T_{in}$  and gas exit pressure  $P_{out}$ . As can be seen, the HX power increased with water mass flow rate and with temperature difference between hot and cold fluid ( $T_c = 274 \text{ K}$ ). For low exit pressures, the power leveled off for  $\dot{m}_{H_2} > 0.8 \text{ kg/s}$ , while at higher pressures the HX power continued to increase with mass flow rate, but seemed

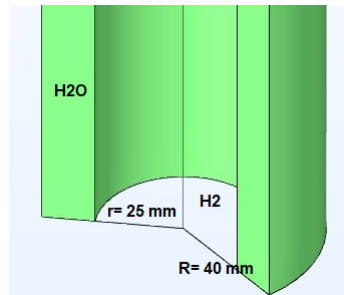


Figure 2: Schematic view of heat exchanger tubes. The thickness of the two steel tubes is 1 mm.

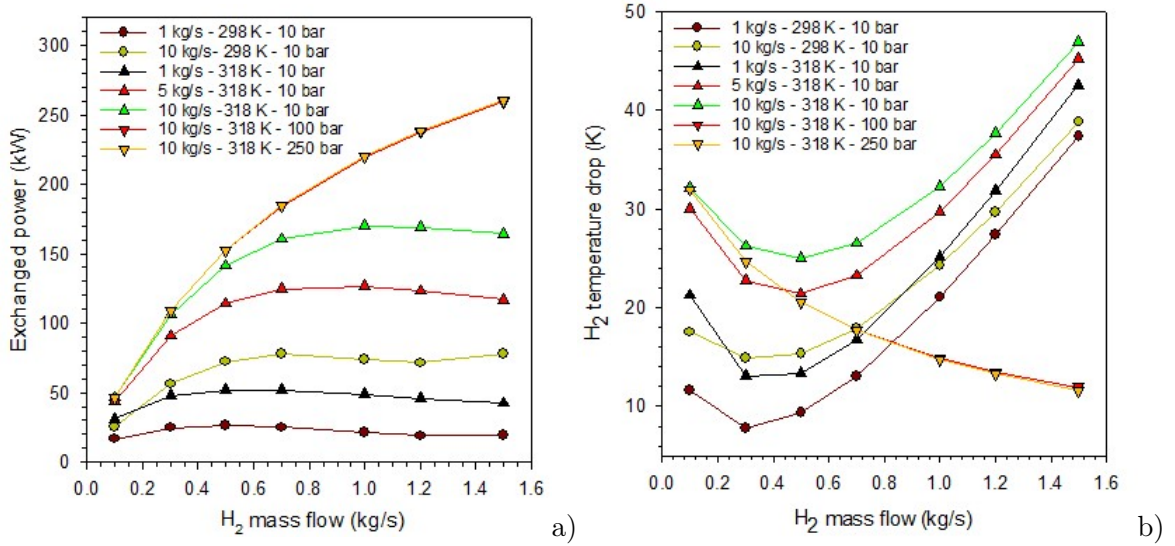


Figure 3: a) Total heat exchange power as function of H<sub>2</sub> mass flow rate for H<sub>2</sub> and b) the corresponding temperature drop in the hydrogen gas. The notation in the legends: Water mass flow rate  $\dot{m}_c$  – H<sub>2</sub> inlet temperature  $T_{in}$  – H<sub>2</sub> exit pressure  $P_{out}$ .

to nearly be independent of the exit pressure.

These results can be seen in a more useful way by looking at the temperature drop  $\Delta T$  over the heat exchanger for the gas as presented in Fig. 3b). For the lowest flow rates,  $\Delta T$  actually decreased with increasing  $\dot{m}_{H_2}$ , indicating that the heat transfer is not efficient. However, in the low pressure range and above  $\dot{m}_{H_2} > 0.5$  kg/s, the HX power increased nearly linearly with flow rate and with temperature drop in the range  $10 \text{ K} \leq \Delta T \leq 40 \text{ K}$ . For higher exit pressures  $P_{out} > 250$  bar, the relatively high density of the gas led to a decrease in the cooling effect, and consequently also a drop in  $\Delta T$ , as the hydrogen flow rate was increased. Here, apparently the heat exchange power increased but not fast enough to compensate for the increasing flow rate.

The effect of increased exit pressure, and thereby density of the gas, can be seen in Fig. 4. At constant flow rate the exchange power  $\dot{Q}$  increased up to a pressure of about  $P_{out} \approx 40$  bar and then was nearly constant as seen in Fig. 4a). However, there was a considerable decrease in the temperature drop  $\Delta T$  of the gas in the low pressure range, mainly due to the increased density as pressure increased, i.e., there was more material to cool down. Above about  $P_{out} = 100$  bar this drop  $\Delta T$  remained constant. Both the heat exchange power and the temperature drop scaled nearly proportional to the hydrogen mass density as one would expect from simple theory of heat exchangers.

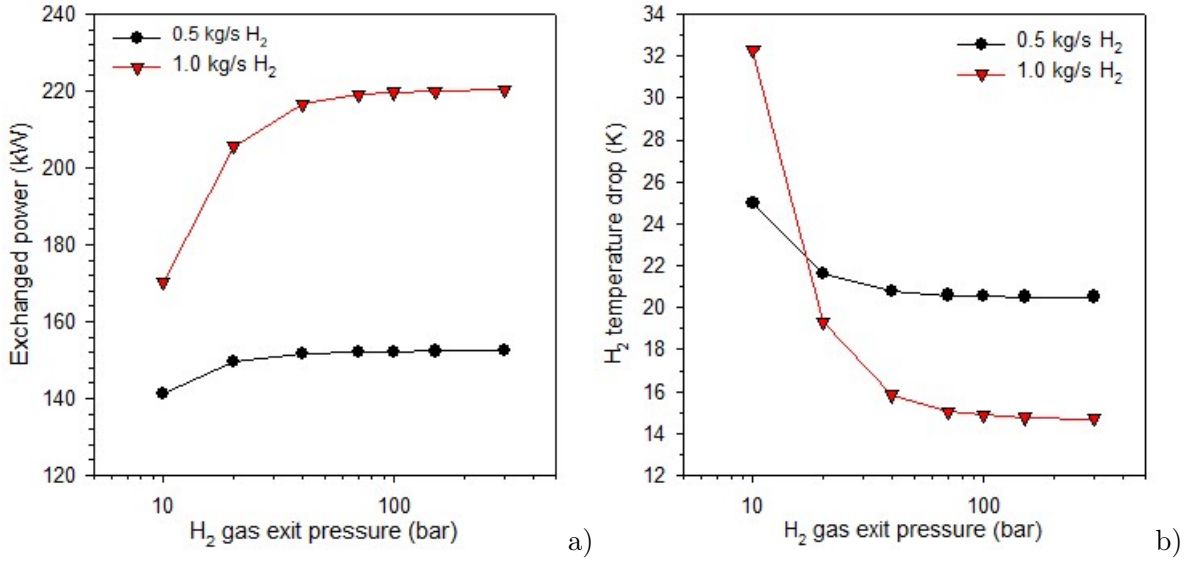


Figure 4: a) Heat exchange power  $\dot{Q}$  as function of hydrogen exit pressure  $P_{out}$  for two flow rates of gas. b) The corresponding drop in temperature of the gas. The values were calculated for a H<sub>2</sub> inlet temperature of  $T_{in} = 318$  K.

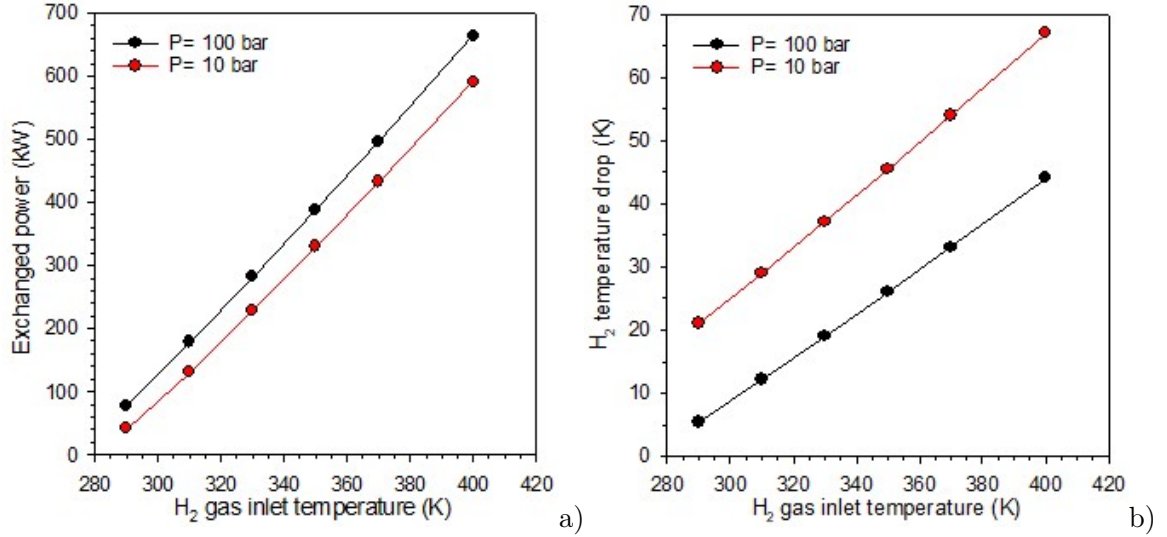


Figure 5: a) Heat exchange power and b) hydrogen gas temperature drop as function of gas inlet temperature  $T_{in}$  for H<sub>2</sub> mass flow  $\dot{m}_{H_2} = 1$  kg/s, water flow  $\dot{m}_c = 10$  kg/s, and  $T_c = 274$  K.

Simulations with varying gas inlet temperature  $T_{in}$  and with water temperature kept fixed at  $T_c = 274$  K showed the expected linear variation with temperature difference  $T_{in} - T_c$  as shown in Fig. 5. A linear fit  $\Delta T \sim \varepsilon \cdot (T_{in} - T_c)$  gave  $\varepsilon = 0.41$  and  $\varepsilon = 0.35$  for  $P_{out} = 10$  bar and 100 bar, respectively (Fig. 5b). Here,  $\varepsilon$  is the same as the effectiveness defined in Eqn. 4, i.e., it gives the the amount of removed heat (power  $\dot{Q}$ ) relative to the maximum possible value. For the cases shown in Fig. 4, the effectiveness was  $\varepsilon \approx 0.47$  for  $\dot{m}_{H_2} = 0.5$  kg/s and  $\varepsilon \approx 0.34$  for  $\dot{m}_{H_2} = 1.0$  kg/s, except for the lowest flow rates where its value was slightly higher.

The heat capacity at constant pressure  $c_p$  (“specific heat”) of hydrogen is in the range  $14.4 \text{ kJ}/(\text{kg} \cdot \text{K}) \leq c_p \leq 14.8 \text{ kJ}/(\text{kg} \cdot \text{K})$  for pressures in range 1 – 300 bar. For water the value is  $c_{p,H_2O} \leq 4.22 \text{ kJ}/(\text{kg} \cdot \text{K})$ . With  $\dot{m}_{H_2} = 1$  kg/s and  $\dot{m}_{H_2O} = 10$  kg/s, the capacity

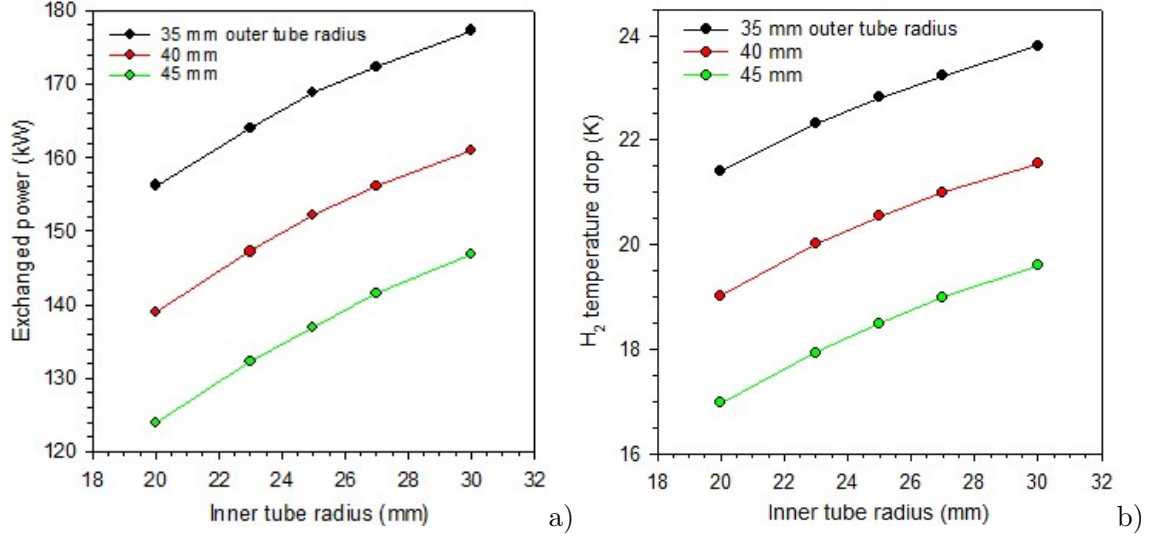


Figure 6: Effect of HX inner tube size on a) exchanged heat power  $\dot{Q}$  and b) temperature drop  $\Delta T$  for various sizes of the water outer tube radius. In all cases the flows were  $\dot{m}_{H_2} = 1$  kg/s and  $\dot{m}_c = 10$  kg/s with  $T_{in} = 318$  K and  $T_c = 274$  K.

ratio defined above was  $C_r = \frac{(\dot{m}c_p)_{min}}{(\dot{m}c_p)_{max}} = \frac{(\dot{m}c_p)_{H_2}}{(\dot{m}c_p)_{H_2O}} \approx \frac{14.6}{42.2} = 0.346$ , and the heat transfer rate and effectiveness were controlled mainly by the flow of hydrogen. Based on Eq. 7, values for  $NTU$  were calculated and were in the range 0.5–0.7. From Eq. 2 the Log-Mean Temperature Difference (LMTD) was found typically to be near  $\Delta T_{lm} \approx 30$ . Then, from the known surface area  $A \approx A_s$  (here  $A = 1.57$  m<sup>2</sup>), the main parameter characterizing the system, i.e. the *effective heat transfer coefficient*  $U$  can be calculated from Eq. 3. This parameter will depend on the flow conditions in the inner and outer tubes and can be used to estimate cooling power  $\dot{Q}$  for similar flow conditions but with different inlet and outlet temperatures. In the simulations presented above, typically  $U = 3000 - 4000$  W/(m<sup>2</sup> · K).

### 3.3 Exploring effects of HX tube sizes

In the above simulations the sizes of the heat exchanger tubes were kept at fixed, chosen values:  $r_i = 25$  mm for the inner,  $r_o = 40$  mm for the outer, and  $L = 10$  m for the length. However, flow conditions in the tubes as well as heat exchange power will depend on sizes. In order to explore how much influence these parameters will have on the performance, the effects of variations of the inner and outer radius of the tubes were studied. The results are presented in Fig. 6. As can be seen, for fixed outer tube radius the heat transfer power as well as the temperature drop increased with inner tube radius (for fixed mass transfer rates  $\dot{m}_{H_2}$  and  $\dot{m}_c$ ). This was probably due to lower gas velocity in m/s inside the inner tube and larger heat transfer surface, which both contributed to more efficient heat transfer. However, a 50% increase in inner radius gives 50% increase in surface area but gave only 10–15% increase in temperature drop. From this figure the  $r_i/r_o$ -combination of 30mm/45mm had the same cooling effect as the combination  $r_i/r_o = 21$ mm/40mm.

Increasing the tube length of a heat exchanger may seem a simple way to increase cooling capacity. But this works only to a limited degree as can be clearly seen in Fig. 7a). Here, the tube length has been increased from  $L = 5$  m up to 100 m. First, there was a nearly linear increase with length for both temperature drop  $\Delta T$  (black curve - left axis) and for cooling

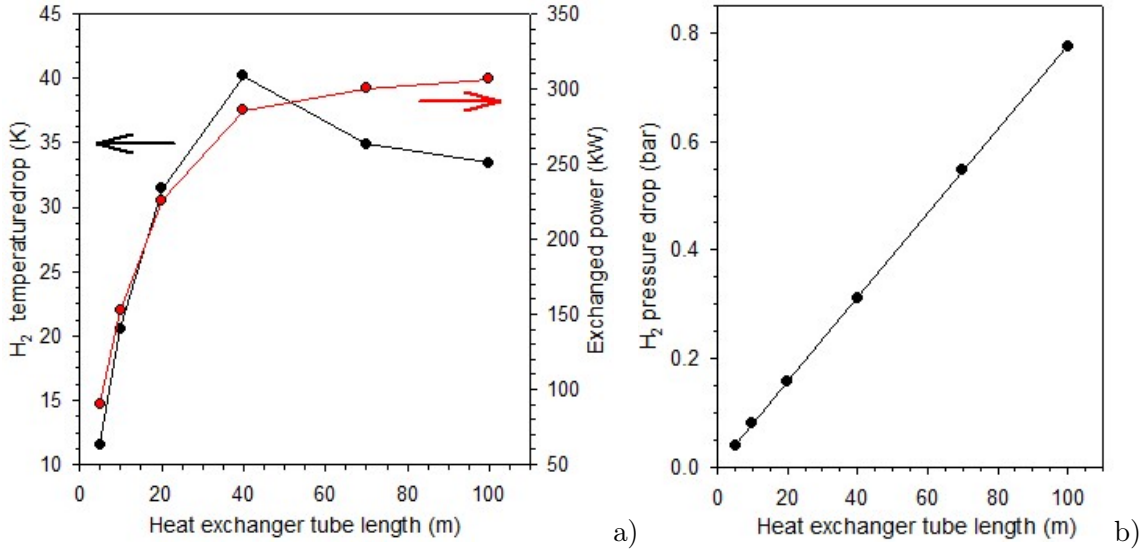


Figure 7: a) Variation of temperature drop  $\Delta T$  (left axis scale) and HX power  $\dot{Q}$  (right axis scale) on tube length  $L$ . b) Pressure drop  $\Delta P$  in gas. Flow conditions:  $\dot{m}_{H_2} = 0.5$  kg/s,  $\dot{m}_c = 10$  kg/s, H<sub>2</sub> exit pressure 100 bar.

power  $\dot{Q}$  (red curve - right axis), but this leveled off to nearly constant (or slightly dropping) beyond  $L \approx 40$  m and reached maximum values of  $\Delta T = 35 - 40$  K and  $\dot{Q} \approx 300$  kW. The gas pressure drop across the heat exchanger remained small ( $< 1$  bar) for these flow conditions as shown in Fig. 7b).

## 4 Discussion - using water as coolant

There are many parameters involved in efficient heat exchanger design and operation, including system sizes (radius, length) and flow conditions (temperature, pressure, mass flow rate), and it is difficult to optimize without having in mind also practical considerations and system cost. Based on initial calculations in EES, a temperature at the HX outlet, i.e., at the inlet to the tank, of about  $T_{h,out} = 233$  K =  $-40$  °C will be needed during fast filling in order to keep the temperature inside the tank below the upper temperature limit of about 80 °C. By adding anti-freeze to water, the freezing point can be reduced a significant amount. For example a mixture of 60% ethylene glycol and 40% water freezes at  $-45$  °C, and has a specific heat  $c_p$  of about 3/4 that of water. The viscosity of such glycol/water mixtures is much higher than that of water, but the glycol/water flow conditions can be kept similar, and then the heat transfer effects may increase due to the larger temperature difference between the gas and the coolant. This option will be discussed in the second part of this report.

As can be deduced from Fig. 5, the temperature drop in the gas scaled with the temperature difference between incoming gas and cooling fluid  $\Delta T_{inlets} = T_{h,in} - T_{c,in}$ . This was as expected from the general theory in Section 2.1. With  $T_{c,in} = 233$  K for the HX fluid mixture, ambient temperature  $T_{h,in} = 25$  °C = 298 K for the gas,  $\varepsilon = 0.45 - 0.50$ , and using  $\dot{m}_c/\dot{m}_h \approx 10$ , a temperature drop up to  $\Delta T = 35$  K can be obtained. For cooling of 1 ton of gas, much more than 10 tons ( $> 10$  m<sup>3</sup>) of cooling fluid need to be prepared and stored before the filling operation. This will require additional infrastructure for storage and pre-cooling.

However, one single double-pipe heat exchanger may not be sufficient to meet the cooling

needs for a medium sized hydrogen gas tank during bunkering. An alternative solution will be to use several pipes of smaller radius, either as parallel pipes or in multi-pass. Then, the total surface area will be increased, flow velocity will be decreased, and heat exchange may be improved. With several thinner pipes in parallel, a total hydrogen mass flowrate of about 1 kg/s and total coolant flowrate only slightly above 10 kg/s may be sufficient to reach the temperature goals. Smaller pipe dimensions will lead to higher pressure drop in the gas. However, the complexities of such multi-pipe systems will clearly increase the installation costs (CAPEX). Part 2 of this report contains simulation studies with glycol/water mixture coolant as well as using reduced pipe dimensions and fluid flowrates that may contribute to partly solve the temperature challenge mentioned above.

It may also be noted that there exist synthetic, organic or silicone based heat transfer fluids that can operate down to  $-100^{\circ}\text{C}$  but these are expensive, and their specific heat is considerably lower than that of water ( $\sim < \frac{1}{5}$ ). Their environmental impact may be hazardous and give considerable drawback to systems involving their use in heat exchangers.

## 5 Conclusion of Part 1

Finite element based computer simulations have been performed for a heat exchanger to be used during filling at moderate to high transfer rates of tanks for compressed hydrogen gas. The model was built in order to give heat transfer rates in the order of a few 100 kW based on cold water as coolant. Temperature drop in the gas of up to about 30 K was obtained. Cooling power of slightly above 200 kW can be obtained in a single counter-flow double pipe heat exchanger. However, more complex design with several parallel pipes may be needed to reach the 500-1000 kW level that probably will be needed for filling in less than one half hour of tanks containing about 1 ton of compressed gas.

# Part 2 - Cooling based on ethylene glycol-water mixtures

## 6 Cooling using other water-based refrigerants

In order to reduce the inlet temperature of the coolant below the freezing point of water ( $0^\circ\text{C}$ ,  $273.15\text{ K}$ ) to achieve a more efficient cooling, solutions of water mixed with organic based liquids can be used. Some examples are mixtures with glycerol ( $T_{min} = -40^\circ\text{C}$ ), ethyl alcohol ( $-45^\circ\text{C}$ ), propylene glycol ( $-50^\circ\text{C}$ ), or ethylene glycol ( $-51^\circ\text{C}$ ). Even ordinary salt, NaCl, can be used ( $T_{min} = -33^\circ\text{C}$ ). However, in order to have a wide temperature range of operation, ethylene glycol-water (EG-water) mixtures are commonly used. Depending on concentration, these mixtures can operate from  $T_{min}$  up to a maximum temperature of about  $T_{max} = 125^\circ\text{C}$ . The concentration range of ethylene glycol can be from few % up to 60%, and this will influence the physical properties of the mixture, in particular the viscosity and heat capacity. Figure 8 shows how the freezing point of an EG-water mixture varies with the EG concentration. Figure 9a) shows how viscosity  $\eta$  and heat capacity  $c_p$  vary with temperature for pure water and for a 50% EG-water mixture. As can be seen, the most important change happens in the viscosity of the fluids at lower temperatures, which for EG-water can change by a factor of more than 100 over its applicable range. As a compromise between lowest freezing point and not too high viscosity, the EG-water-50% mixture was used as a typical example in the rest of this study.

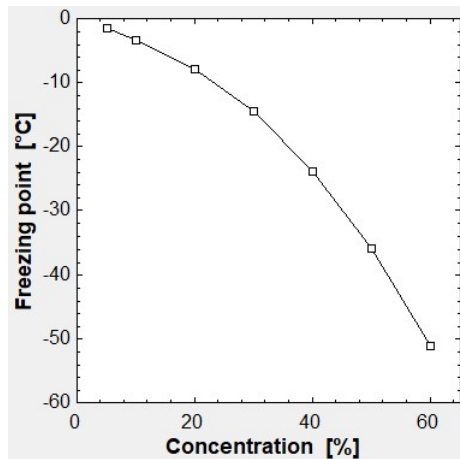


Figure 8: The freezing temperature of ethylene glycol-water mixtures as function EG concentration.

In a fluid flow model, the other important parameters in addition to  $\eta$  and  $c_p$ , are fluid density  $\rho$  and heat conductivity  $\kappa$ . The temperature variation of these parameters are presented in Fig. 9b). These changes with temperature have also to be taken into considerations in the flow simulation model. Based on data for EG-water-50% mixtures extracted from Ref. [4], the following parameterizations were found to be valid in the temperature range  $238\text{ K} < T < 400\text{ K}$ :

$$\eta(T)/[\text{Pa} \cdot \text{s}] = 1.089 \cdot 10^{-3} + 1.783 \cdot 10^5 \cdot \exp(-0.0628 \cdot T) \quad (8)$$



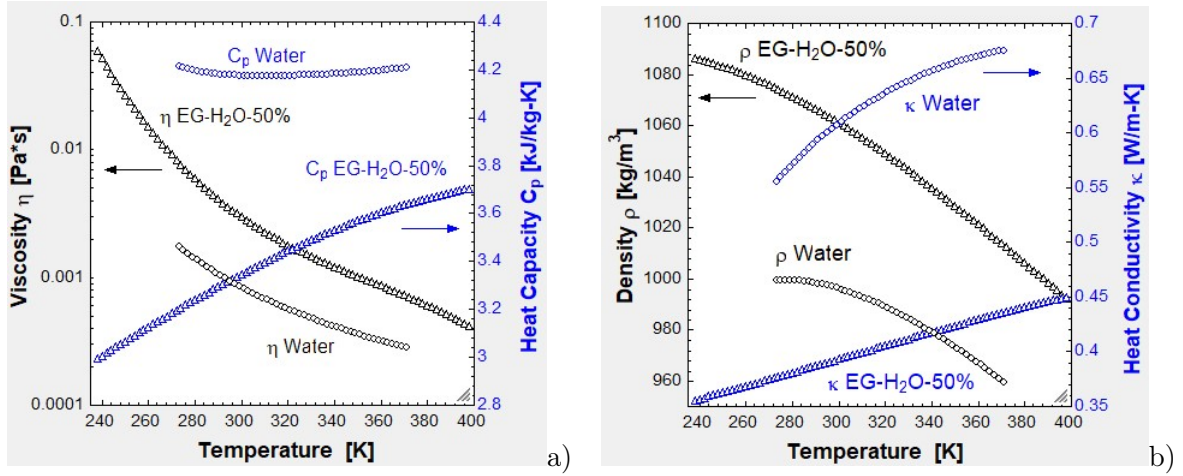


Figure 9: Properties of pure water and an EG-water mixture. a) Viscosity  $\eta$  and heat capacity  $c_p$  as function of temperature. Note log scale on left hand axis. b) Density  $\rho$  and heat conductivity  $\kappa$  vs. temperature.

$$c_p(T)/[\text{kJ}/(\text{kg} \cdot \text{K})] = 0.629 + 0.0131 \cdot T - 1.35 \cdot 10^{-5} \cdot T^2 \quad (9)$$

$$\rho(T)/[\text{kg}/\text{m}^3] = 1070.6 + 0.476 \cdot T - 1.7 \cdot 10^{-3} \cdot T^2 \quad (10)$$

$$\kappa(T)/[\text{W}/(\text{m} \cdot \text{K})] = 0.2142 + 5.965 \cdot 10^{-4} \cdot T \quad (11)$$

These parameterizations were supplied to the material properties library of the COMSOL software to be used in the following simulations.

## 7 Comparisons of efficiency of water and EG-water as coolant

Several series of simulations were performed using either an EG-water-50% mixture or pure water as coolant in the HX-model above (inner tube  $r_i = 25$  mm, outer tube  $r_o = 24$  mm, length  $L = 10$  m - see Fig. 2). The hydrogen gas exit pressure was kept fixed at  $P_{out} = 100$  bar. Similar simulations were also done on two smaller systems, both of length  $L = 10$  m, but with inner/outer tube dimensions  $r_i/r_o = 15$  mm / 24 mm and  $r_i/r_o = 10$  mm / 15 mm. Various values of the mass flowrate of the coolants in the range  $0.02$  kg/s  $< \dot{m}_c < 10$  kg/s were explored. Different flowrates of gas in the range  $0.005$  kg/s  $< \dot{m}_{H_2} < 1.0$  kg/s were used.

The drop in temperature of the gas,  $\Delta T$ , is proportional to the total amount of exchanged heat  $Q$ . For a certain flowrate  $\dot{m}_{H_2}$ ,  $\Delta T$  is also proportional to the heat exchange rate  $\dot{Q}$ . Using Eq. 3, the heat exchange coefficient  $U$  will then be the important parameter that determines the exit temperature  $T_{out}$  and temperature drop  $\Delta T$  for fixed gas inlet temperature  $T_{in}$  and fixed temperature of the coolant  $T_c$ . In the following, we used  $T_c = 238$  K for EG-water and 274 K for pure water. The results for the effective value of  $U$  from selected simulations are presented in Table 1. Here, the left column shows the type and temperature of coolant, and the second column coolant mass flowrate. The next columns show heat exchange coefficients for systems with different sizes of the inner and outer tubes,  $r_i$  and  $r_o$ . As can be seen, the effective heat transfer is apparently much better for water than for EG-water mixtures under the same flow conditions – nearly a factor of four, and more than five times for the widest tubes. Some reasons for this will be discussed in the next section. However, this better cooling capacity of water is partly compensated for by the lower temperature  $T_c$  of the

	$R_i/R_o=$	25/40 mm	15/24 mm	10/15 mm
Coolant / $T_c$	$\dot{m}_c$ [kg/s]	$U$ [W/(m <sup>2</sup> ·K)]	$U$ [W/(m <sup>2</sup> ·K)]	$U$ [W/(m <sup>2</sup> ·K)]
Water / 274 K	1	1111	2486	5766
EG-H2O / 238 K	1	203	512	1292
Water / 274 K	2	1593	3955	8232
EG-H2O / 238 K	2	285	826	1989
Water / 274 K	5	2443	6361	12043
EG-H2O / 238 K	5	451	1436	3536

Table 1: Comparison of effective heat transfer coefficient  $U$  for water and EG-H2O-50% coolants for selected coolant mass flowrates  $\dot{m}_c$  for heat exchangers with different radius of inner/outer tubes. The hydrogen mass flowrate was  $\dot{m}_{H_2} = 0.5$  kg/s and the gas inlet temperature  $T_{in} = 300$  K.

EG-water coolant. Then, the final temperature drop in the gas may be similar. Also, the cooling capacity increases with decreasing tube radius as is clearly seen in the table. This can partly be explained by the increasing flow velocities of fluids for reduced tube cross sections and partly due to the effect that a thinner inner tube brought more of the gas closer to the cold inner tube wall.

The effective heat transfer coefficient will depend on the mass flowrate of the coolant. Figure 10 shows how the heat transfer of water and EG-water depends on coolant flowrate  $\dot{m}_c$  for differently sized pipes [25 mm - a) and c), 15 mm - b) and d)]. As one may expect from Eq. 3, the heat transfer coefficient is independent of the temperature  $T_{in} = T_{H_2}$  of the incoming gas, as demonstrated in Figs. 10 a) and b). The actual drop in temperature of the gas,  $\Delta T$ , in these two cases are shown in Figs. 10 c) and d). The slightly larger temperature drop using EG-water was due to the lower coolant temperature  $T_c = 238$  K as compared to  $T_c = 274$  K for water. One may note that the differences in  $\Delta T$ -values between the coolants were smaller at low coolant flowrates and increased at higher flowrates.

The effect of the HX design on the cooling capacity and temperature drop can be more clearly seen in Fig. 11, which shows a comparison of one narrow tubes and one wider tubes counter-flow heat exchanger. Here, the inner tube radii were  $r_i = 15$  mm and  $r_i = 25$  mm, respectively. Although the HX-coefficients  $U$  for EG-H2O systems were much smaller than those for systems based on pure water, for narrower tube systems the temperature drop in the gas was larger with EG-water-50% then with pure water. This was mainly due to the lower coolant temperature  $T_c$ , and the differences between the coolants became smaller as the gas temperature rose as shown in Fig. 11a). However, for wider tube HX-systems this effect appeared to be opposite as shown in Fig. 11b). Here water was a much better coolant then EG-water mixtures, and the differences between coolants increased as gas inlet temperature  $T_{in}$  increased. Some of the explanation for this different behaviour will be discussed in the following section about coolant flow patterns.

Table 2 shows typical values of the heat transfer coefficient in the narrow tube system for smaller gas mass flowrates with fixed coolant flowrate  $\dot{m}_c = 3$  kg/s. These values were found to be nearly independent of the gas exit pressure  $P_{out}$  from the HX.

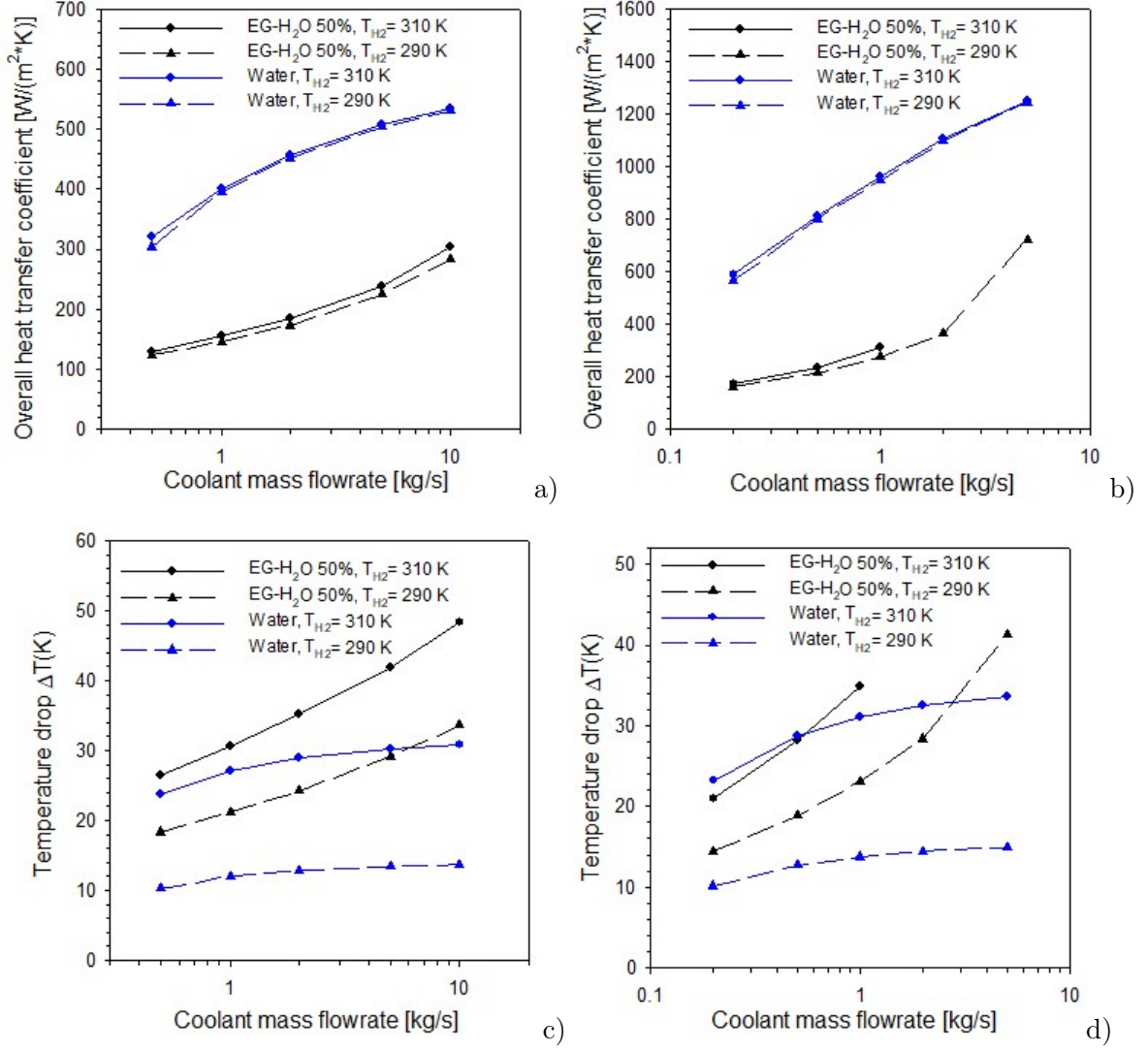


Figure 10: Heat transfer coefficients ( $U$  in Eq. 3) as function of coolant mass flowrate for heat exchangers with inner tube radius a)  $r_i = 25$  mm and b)  $r_i = 15$  mm for fixed H<sub>2</sub> flowrate of  $\dot{m}_{H_2} = 0.03$  kg/s = 1.8 kg/min. The corresponding temperature drop  $\Delta T$  in the gas for the two different radii are shown in c) - 25 mm and d) - 15 mm. The gas inlet temperatures were  $T_{in} = 290$  K or 310 K.

	Water	EG-H2O-50%
$\dot{m}_{H_2}$ /kg/s	$U$ [W/(m <sup>2</sup> ·K)]	$U$ [W/(m <sup>2</sup> ·K)]
0.03	1200	520
0.1	2400	810
0.3	3900	1000

Table 2: Effective heat transfer coefficient  $U$  for water and EG-water mixtures in a HX-system with inner/outer tube radius of 15 mm / 24 mm and coolant flowrate  $\dot{m}_c = 3$  kg/s.

For fixed values of the flowrates of gas and coolant and keeping fixed separation of the inner and outer tube (i.e., fixed  $r_o - r_i = 5$  mm), the heat transfer coefficient decreased with increasing inner tube radius as shown in Fig. 12. This decreasing trend may partly be due to the lower velocities of gas and coolant as the cross section areas available to the fluids increased. The  $U$ -values for pure water were typically 70-100 % higher than those for the EG-water mixture.

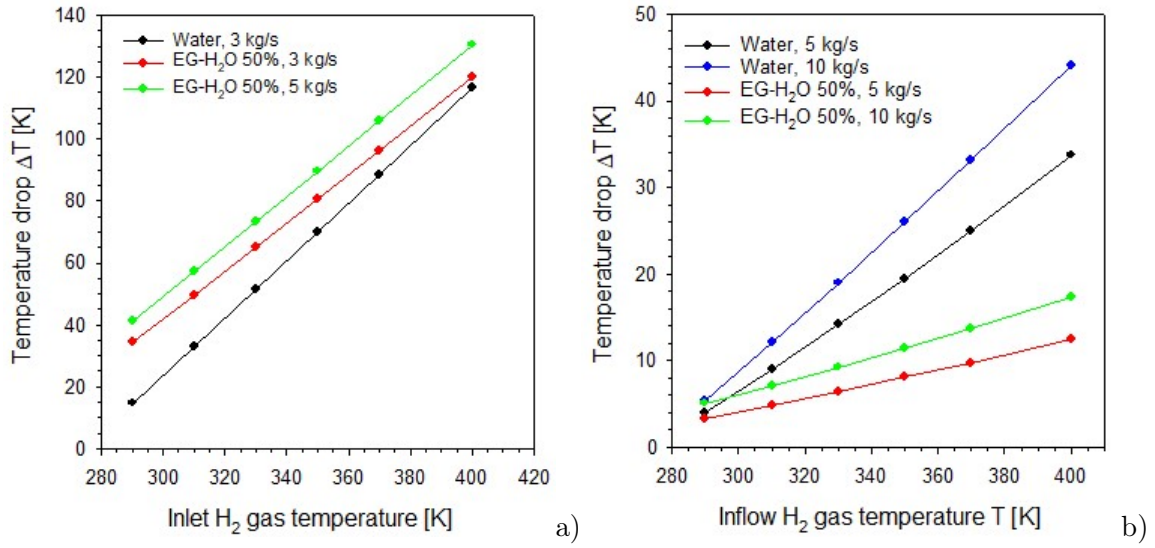


Figure 11: a) Temperature drop in the hydrogen gas as function of gas inlet temperature for different type and flowrate  $\dot{m}_c$  of coolant. a) HX-system with inner/outer tube radius of 15 mm / 24 mm, and b) for  $r_i / r_o = 25$  mm / 40 mm. Here  $\dot{m}_{H_2} = 0.03$  kg/s and  $P_{out} = 100$  bar.

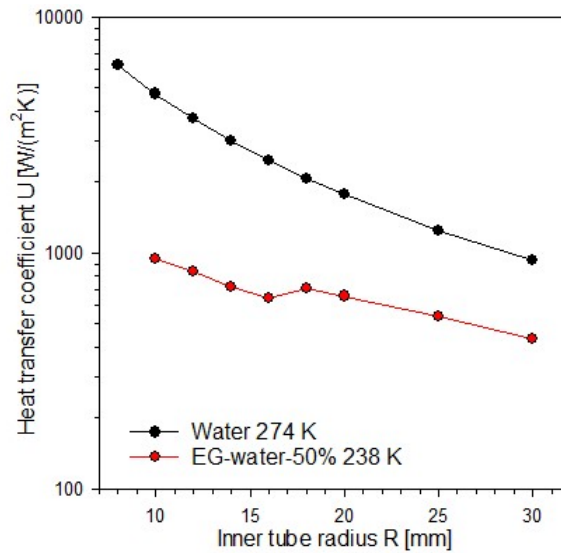


Figure 12: Variation of heat transfer coefficient  $U$  with radius  $r_i$  of inner tube for fixed separation between the tubes,  $r_o - r_i = 5$  mm. The flowrates were kept constant at  $\dot{m}_{H_2} = 0.1$  kg/s and  $\dot{m}_c = 2.0$  kg/s.

## 8 Coolant flow patterns and cooling capacity

As discussed above, the dimensions of heat exchanger tubes have important effects on their cooling capacity. This will be described in more details in this section.

### 8.1 Flow velocity and pressure drops

The flow velocity  $v_g$  of gas will depend on the tube diameter, exit pressure and on the mass flowrate of the gas. Typically, it ranged from  $v_g \leq 5$  m/s up to several hundreds of m/s. The velocity of the coolants was in the range  $0.1 \text{ m/s} < v_{cool} < 4 \text{ m/s}$ . The Reynolds number characterizing the flow is defined as  $Re = \frac{\rho v d}{\eta}$ , where  $v$  is the flow velocity and  $d$  is a typical length scale (e.g. tube radius or distance between tubes). For the hydrogen gas, we found  $1500 < Re_{H_2} < 2 \cdot 10^7$ , and for water and EG-water-50% the numbers were in the range  $30 < Re_{H_2O} < 7 \cdot 10^4$  and  $1.0 < Re_{EG-H_2O} < 2000$ , respectively. The flow were then in most cases turbulent both for the hydrogen gas and for the water coolant. This has been taken into account in the simulations and ensured a good mixing of hot and cold parts of the fluids. However, for EG-based coolant the flow will mainly be laminar, and the temperature mixing during flow will be less efficient.

The pressure drop  $\Delta P_{cool}$  driving the coolant was typically a fraction of 1 bar, but for coolant flowrate near 10 kg/s the pressure drop over the 10 m long tube could go above 1.0 bar. The pressure drop in the gas was often few tens of Pascals but could reach up to about  $\Delta P_{H_2} \approx 0.3$  bar for the highest flowrates.

### 8.2 Velocity and temperature distributions

Although the heat capacity of EG-water mixtures is only about 2/3 of that of water, the most important differences occurred due to the much larger differences in their viscosity and the influence of viscosity on the liquid flow pattern and flow velocity. These effects could be seen when looking into flow and temperature distribution patterns in the CFD simulations. Figure 13 shows some examples of coolant velocity profile at the outlet (left column) and temperature profile plot in a cross section of the annulus of the outer tube (right column). Subfigure 13a)-d) are from wider HX-systems and e)-f) are from a narrower setup.

The water velocity profiles ( $v_{cool}$  vs.  $r$ ) along the outer tube radius near the water outlet showed a nearly parabolic shape in all simulations with only minor differences between the velocity at the inner and outer walls of the annulus (at  $r \approx 25$  mm and 40 mm) as can be seen in Fig. 13a). The heat from the gas was mixed into the whole volume of water before reaching the coolant exit, as shown in Fig. 13b). Here, the water inlet is at the figure “top” at  $z = L = 10$  m and the outlet is at the “bottom” at  $z = 0$  (at the hydrogen gas inlet). The flow mixed well the warmer water from near the wall into the bulk volume of the coolant.

For a similar heat exchanger using EG-water mixture, the situation was somewhat different. Due to the higher viscosity of the EG-H<sub>2</sub>O-50% mixture ( $\eta = 0.06$  Pa·s vs. 0.002 Pa·s for H<sub>2</sub>O), the flow profile in the radial direction inside the annulus became very asymmetric and skewed as seen in Fig. 13c). Near the wall that separated the gas and coolant and close to the coolant exit ( $z = 0$ ), the velocity of the mixture was about five times higher than near the outer wall of the tube (i.e., 1 m/s vs. 0.2 m/s). The strong shear forces near the inner wall did not mix the heat into the bulk of the EG-water mixture, but only a thinner layer

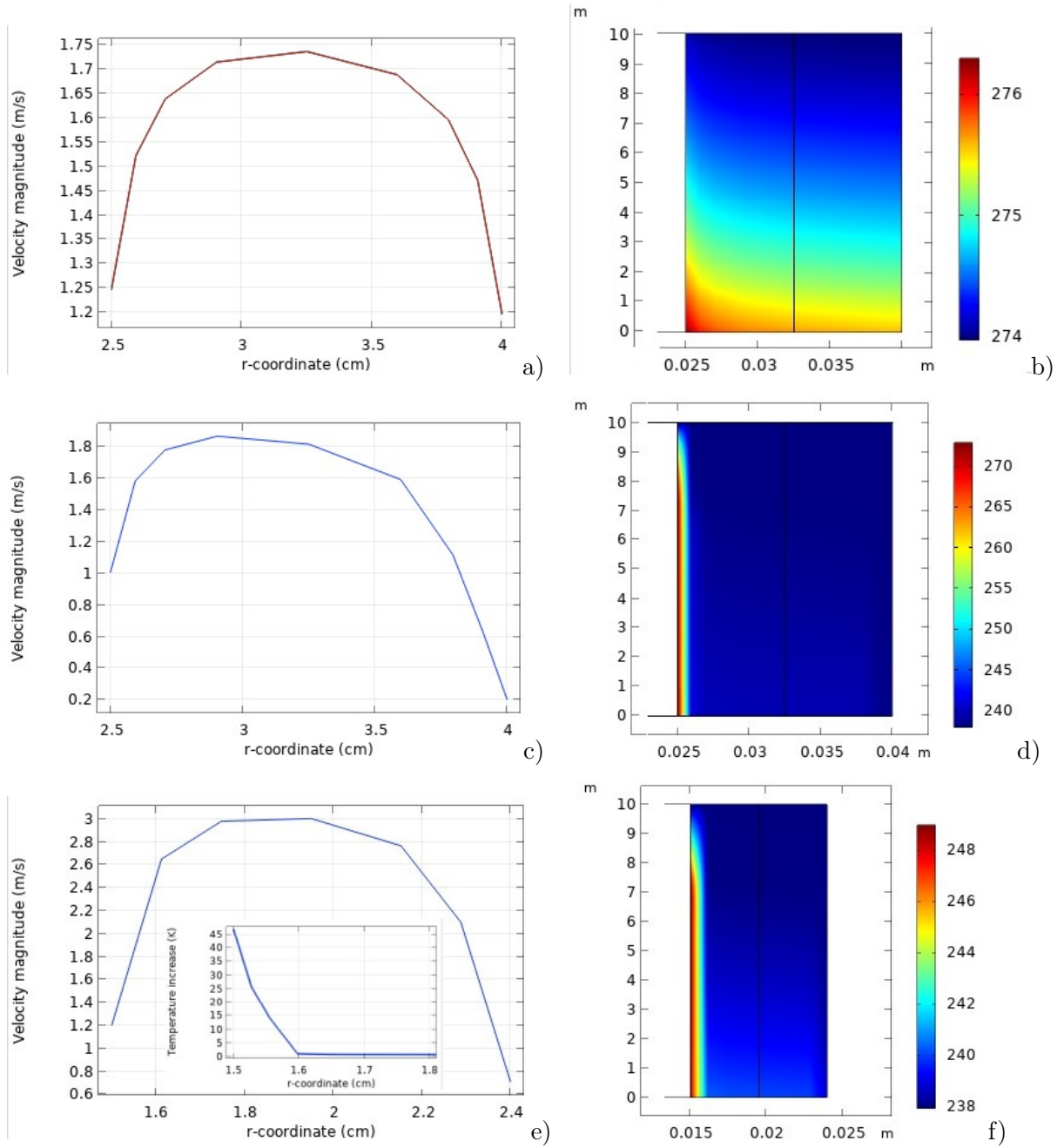


Figure 13: Coolant velocity profiles  $v_{cool}(r)$  at outlet and temperature distributions  $T(r, z)$  inside the coolant for **a)-b) pure water** at 274 K and **c)-f) EG-water-50%** at 238 K. The parameters used in simulation were: a)-b)  $r_i = 25$  mm,  $r_o = 40$  mm,  $\dot{m}_c = 5$  kg/s,  $\dot{m}_{H_2} = 0.06$  kg/s; c)-d)  $r_i = 25$  mm,  $r_o = 40$  mm,  $\dot{m}_c = 5$  kg/s,  $\dot{m}_{H_2} = 0.1$  kg/s; e)-f)  $r_i = 15$  mm,  $r_o = 24$  mm,  $\dot{m}_c = 3$  kg/s,  $\dot{m}_{H_2} = 0.03$  kg/s. In b), d) and f) the coolant inflow was from top of the page (at  $z = L = 10$  m). The temperature of the gas flowing in opposite direction to that of coolant (from  $z = 0$ ) was  $T_{H_2} = 310$  K. The inset in e) shows the temperature increase -  $\Delta T$  vs.  $r$  - in the coolant in a layer of thickness 3 mm closest to the inner wall.

near this wall (of order a few mm) was heated and contributed to the cooling of the gas. This is shown in Fig. 13d).

This uneven heat distribution in the coolant may partly be diminished by using smaller diameters of both inner and outer tubing. One such case with  $r_i/r_o = 15\text{ mm}/24\text{ mm}$  is shown in Figs. 13e) and f). Now the coolant velocity profile was more parabolic in shape (but still slightly asymmetric) and the overall cooling effect with EG-water became better than with pure water, as was also shown in Fig. 11a) above. However, still only the part of the EG-water mixture closer to the wall contributed to the cooling. This can easily be seen in Fig. 13f). This strong temperature gradient in the fluid is displayed more clearly in the inset of Fig. 13e), which shows  $\Delta T$  vs. radius  $r$  in the annulus. Closest to the wall the temperature of the EG-water coolant was increased by about 45 K, and this temperature increase dropped to nearly zero within the first mm closest to the inner wall.

The smaller distance between inner and outer tube in this last case contributed to an effective increased coolant flow velocity, to the improved total cooling effect, and to the larger temperature drop  $\Delta T$ . Indeed, keeping inner tube radius fixed while reducing the outer tube radius, the effective cross section area available for the coolant flow could be reduced. However, a 50% reduction in cross section area with a similar reduction in the mass flowrate, i.e. keeping the flow velocity constant in a thinner annular shell, did only reduce the heat transfer coefficient  $U$  by about 10%. This observation supports what was concluded above that the main cooling effect for EG-water coolants happened in a thin layer of few mm thickness outside the inner tube, and heat will not be distributed throughout the bulk of this coolant. For pure water coolant, the good liquid mixing in the turbulent flow distributed the extracted heat throughout the whole volume of water.

These observations are consistent with what can be deduced from the Prandtl numbers for these fluids. The Prandtl number  $Pr = c_p \eta / \kappa$  is the ratio of momentum diffusivity to thermal diffusivity. Here,  $Pr = 0.7, 13,$  and  $504$  for  $\text{H}_2$ , water, and EG-H<sub>2</sub>O-50%, respectively. This means that for hydrogen the low viscosity will enhance the spreading of heat, while for EG-mixtures with high value of  $Pr$ , heat will mainly be transported by convection. Since convection was small in the relatively fast-flowing EG-mixture with no turbulent mixing, the transport of heat perpendicular to the flow direction was small. Thus, it will be the coolants that limit the heat transport rate in this type of heat exchanger.

## 9 Temperature estimates based on heat transfer coefficients

The effective heat transfer coefficient  $U$  is nearly independent of the temperature and pressure of the incoming gas and only depends on the type of coolant and the mass flowrates  $\dot{m}_{\text{H}_2}$  of gas and  $\dot{m}_c$  of coolant. The total cooling effect depends also of the total contact area  $A_s = 2\pi R_i \cdot L$ , where  $L$  is the length of the HX tubes.

Using Eqns. 2 and 3 or Eqns. 4 and 7, the hydrogen gas exit temperature and temperature drop in the HX could be calculated when inlet temperatures and the  $U$ -value of the flow configuration were known. This can for example be done using the EES software [4]. One example based on a parameterization of  $U$  as function of coolant flowrate  $\dot{m}_c$  for fixed gas flowrate  $\dot{m}_{\text{H}_2}$  is shown in Fig. 14. This figure shows a comparison of the cooling effect of EG-water and pure water for various temperatures of the inlet hydrogen gas temperature.

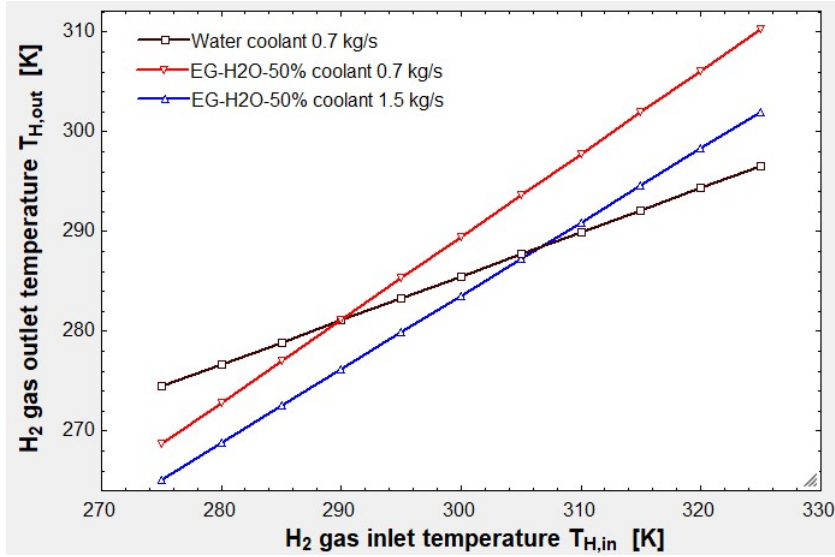


Figure 14: Gas outlet temperature  $T_{H,out}$  from heat exchanger as function of inlet temperature using pure water coolant at ( $\dot{m}_c=0.7$  kg/s,  $T_c=274$  K) and EG-H2O-50% at ( $\dot{m}_c=0.7$  and 1.5 kg/s,  $T_c=238$  K). The hydrogen flowrate was  $\dot{m}_{H_2}=0.1$  kg/s.

The mass flowrate of gas was  $m_{H_2}=0.1$  kg/s and for water the flowrate was  $\dot{m}_c=0.7$  kg/s. Two different flowrates, 0.7 kg/s and 1.5 kg/s, were used for EG-H2O-50%. This figure shows that the cooling effect of the EG-mixture is better than that of water for lower gas inlet temperatures, i.e. up to about  $T_{H,in} \approx 290$  K for similar mass flowrates  $\dot{m}_c=0.7$  kg/s (red curve). Above that temperature pure water was a better coolant. This crossover point can be shifted to higher temperature by increasing the EG-mixture flowrate as shown by the blue curve for  $\dot{m}_c=1.5$  kg/s. Thus, whether EG-H2O-50% or pure water is the best coolant will depend on the details of heat exchanger design and fluid flowrates and will also depend on operation temperature range.

Three different sized counter-flow HX systems have been studied; one with narrow inner tube -  $r_i=10$  mm, one intermediate sized with  $r_i=15$  mm, and one wider with  $r_i=25$  mm. More details and heat exchange coefficient for these systems using water and EG-water coolants can be found in Appendix A. Fig. 15a) shows a summary of some results from calculations of temperature inside a  $5\text{ m}^3$  hydrogen gas tank after a filling of 150 kg gas using the three differently sized HX systems. Coolant flowrates in the range  $0.5\text{ kg/s} < \dot{m}_c < 5\text{ kg/s}$  were used. Here it can clearly be seen that for water coolant the size of the HX tubing is not very important for the final gas temperature. However, for EG-water coolant there is a much wider spread in gas exit temperature and smaller sizes of the tubing have large positive effects on performance.

The final temperature in after filling of 150 kg hydrogen in the same  $5\text{ m}^3$  tank using different coolant flowrates are shown in Fig. 15b). Here, the differently coloured curves are for different gas flowrate and for different type of coolant. In this example there were only smaller differences in the temperature inside the tank for coolant flowrates below about  $\dot{m}_c=0.5$  kg/s. However, these final temperatures are far too high for what can be allowed inside a composite materials tank. In this calculation the EES modeling tool described in Appendix B was used, which also took into account the estimated heat capacity of the tank walls. For coolant flowrates above  $\dot{m}_c \approx 2$  kg/s, there is a clear advantage of using the EG-water coolant



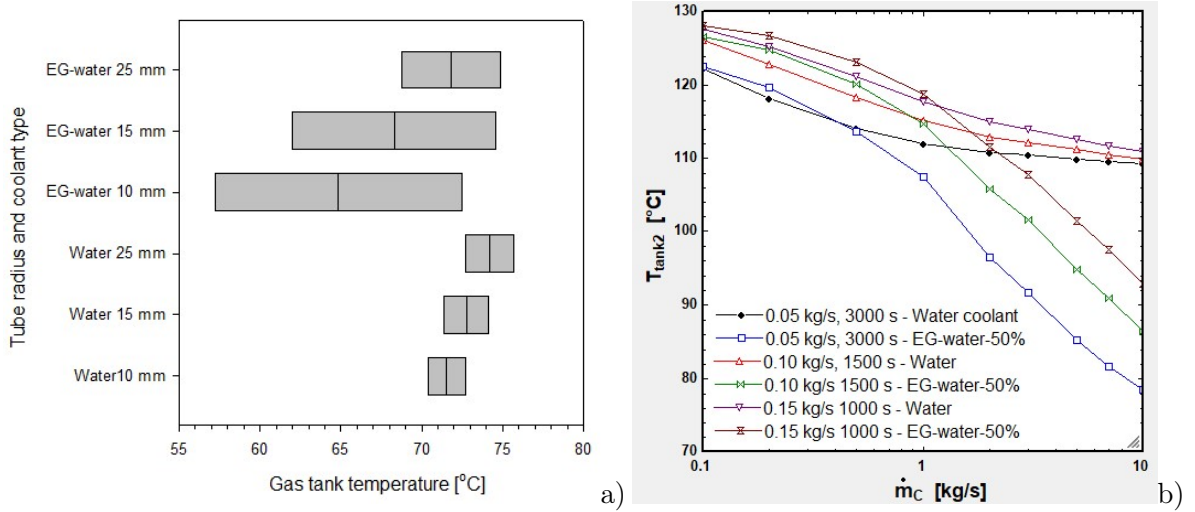


Figure 15: a) Comparison of heat exchangers with different inner tube radius (10/15/25 mm). The bars show ranges of gas temperatures inside a  $5 \text{ m}^3$  tank during filling of  $150 \text{ kg H}_2$  using filling rate of  $0.05 \text{ kg/s}$  ( $3 \text{ kg/min}$ ) for  $1500 \text{ s}$  with i) water at  $1^\circ\text{C}$  or ii) EG-H<sub>2</sub>O-50% at  $-35^\circ\text{C}$  as coolant. The coolant mass flowrates were varied in the range  $0.5\text{-}5.0 \text{ kg/s}$ . b) Final temperature in this tank as function of coolant flowrate  $\dot{m}_c$  using different gas flowrates  $\dot{m}_{H_2}$ . Initial state of the tank was at  $T = 25^\circ\text{C}$ ,  $P = 20 \text{ bar}$ , and the final pressure after filling ended in the range  $62\text{-}70 \text{ bar}$  (depending on final temperature).

with a temperature reduction in the gas  $20\text{-}30 \text{ K}$  larger than that obtained using water. The cooling capability of water seems to level off and be nearly independent of flowrate for  $\dot{m}_c > 5 \text{ kg/s}$  in the current heat exchanger model.

## 10 Summary and Conclusion of Part 2

Various mixtures of ethylene glycol in water can be used as an alternative to pure water in heat exchangers. The temperature of the coolant can then be brought down below  $-50^\circ\text{C}$ . However, due to the much higher viscosity EG-water mixtures, at low temperatures up to 200 times that of pure water, the effectiveness and usefulness of these mixtures show limitations. Higher heat capacity and better flow properties of water make the effective heat transfer coefficient  $U$  of water typically a factor of 2-5 larger than that of EG-water mixtures. This lower value of  $U$  can partly be compensated for by a much lower coolant inlet temperature,  $T_c \ll 0^\circ\text{C}$ . As a general rule, it seems that water appears to be better coolant for large flowrates of gas, which also requires high flowrate of coolant. This can partly be explained by the observation that whereas the whole bulk volume of water is heated during the passage through the heat exchanger, only a thinner layer near the contact wall between the fluids will be heated when using EG-water mixtures. The thickness of this layer can be of order few mm up to about  $5 \text{ mm}$ . Then, a smaller separation between inner tube and outer tube, i.e., the “annulus” for coolant, may be advantageous since the effective flowrate can be reduced without compromising much on the cooling capacity. On the other hand, this will require a higher coolant pressure difference across the heat exchanger tube, adding to system operation costs.

The pressure drop in the inner gas tube was typically less than  $1 \text{ bar}$  for the dimensions of inner tubes studied in the present simulations. The Reynolds numbers  $Re$  for the flow in both

inner and outer tube were in most cases high ( $\sim 10^3 - 10^5$ ), which indicates turbulent flow and improved mixing in the fluid. However, for ethylene glycol-water mixtures it was observed that the  $Re$  numbers are smaller, and the flow was laminar with less efficient temperature mixing. This was confirmed by observing rapid drop in the coolant temperature in a few mm layer outside the wall of the inner tube.

Since the heat transfer coefficient  $U$  depends on the HX system dimensions and fluid flowrates, tables of  $U$ -values for selected system configurations may be created, or the heat transfer coefficient may be parameterized as function relevant system parameters ( $r_i, r_o, \dot{m}_c, \dot{m}_{H_2}, T_c$ ). The effects on  $U$  of gas outlet pressure  $P_{out}$  and gas inlet temperature  $T_{H_2,in}$  were found to be relatively small.

For smaller hydrogen mass flowrates  $\dot{m}_{H_2} \sim 0.1$  kg/s = 6 kg/min, both water and EG-H<sub>2</sub>O-50% coolants with flowrates of  $\dot{m}_c \sim 1$  kg/s can be used in order to keep the outlet gas temperature below about 25 °C. However, to fill larger tanks with one ton or more of gas in about one half hour, then the much higher gas flowrates that will be needed will require a special and optimized design of the heat exchanger in order to avoid overheating.

This report has just discussed heat transfer in simple, unmodified double pipe heat exchangers. There exists a large literature on how passive or active modifications of such devices can improve heat transfer, including tube inserts, wall modifications and stirrers to get better flow mixing. This is summarized in a review article from 2017 by M. Omid, M. Farhadi, and M. Jafari [9]. Some studies published after that are given in Refs. [10]–[17]. Use of nanoparticles added to the coolant in order to increase the thermal coupling has also been studied, and this has been summarized by Hajatzadeh et al. [18] and by Louis et al. [19]. All these types of modifications can increase the heat transfer rate by a considerable amount but will also increase the pressure drop across the tubing and thereby the pumping power needed. Thus, there is an energy cost for all such improvements. Finally, a compressed hydrogen storage system for fast filling of hydrogen gas has been studied by Li et al. [20].

## References

- [1] The H2Maritime project - <https://ife.no/en/hydrogen-in-the-maritime-sector/>
- [2] The Joule-Thomson effect - [https://en.wikipedia.org/wiki/Joule-Thomson\\_effect](https://en.wikipedia.org/wiki/Joule-Thomson_effect)
- [3] SAE J 2601-2-2014 protocol, *Fueling Protocol for Gaseous Hydrogen Powered Heavy Duty Vehicles*, [https://www.sae.org/standards/content/j2601/2\\_201409/](https://www.sae.org/standards/content/j2601/2_201409/)
- [4] Engineering Equation Solver - <https://fchartsoftware.com/>
- [5] J.H. Lienhard IV and J.H. Lienhard V, *A Heat Transfer Textbook* (Phlogiston Press, Cambridge, MA, 2020), <https://ahtt.mit.edu/>
- [6] D. Taler, *Numerical Modelling and Experimental Testing of Heat Exchangers*, (Springer, 2019) ISBN 978-3-319-91128-1
- [7] O. Levenspiel, *Engineering Flow and Heat Exchange*, (Springer, 2014) ISBN 978-1-4899-7454-9
- [8] Comsol Multiphysics - <https://www.comsol.com/>

- [9] M. Omidi, M. Farhadi, and M. Jafari, *A comprehensive review on double pipe heat exchangers*, Applied Thermal Engineering, **110**, 1075 (2017)
- [10] M. Hashemian et al., *Enhancement of heat transfer rate with structural modification of double pipe heat exchanger by changing cylindrical form of tubes into conical form*, Applied Thermal Engineering, **118**, 408 (2017)
- [11] R. Hosseini-zhad et al., *Numerical study of turbulent nanofluid heat transfer in a tubular heat exchanger with twin twisted-tape inserts*, Journal of Thermal Analysis and Calorimetry, **132**, 741 (2018)
- [12] A. Peccini et al., *Optimal design of double pipe heat exchanger structures*, Industrial and Engineering Chemistry Research, **58**, 12080 (2019)
- [13] M Ali and R. Jalal, *Experimental investigation of heat transfer enhancement in a double pipe heat exchanger with a twisted inner pipe*, Heat Transfer, **50**, 8121 (2021)
- [14] T. Dagdevir and V. Ozceyhan, *An experimental study on heat transfer enhancement and flow characteristics of a tube with plain, perforated and dimpled twisted tape inserts*, International Journal of Thermal Sciences, **159**, 106564 (2021)
- [15] L. Wang, Y. Lei and S. Jing, *Performance of a Double-Tube Heat Exchanger with Staggered Helical Fins*, Chemical Engineering and Technology, **45**, 953 (2022)
- [16] Q. Hu et al., *Experimental and numerical investigation of turbulent heat transfer enhancement of an intermediate heat exchanger using corrugated tubes*, International Journal of Heat and Mass Transfer, **185**, 122385 (2022)
- [17] S. Marzouk et al., *A comparative numerical study of shell and multi-tube heat exchanger performance with different baffles configurations*, International Journal of Thermal Sciences, **179**, 107655 (2022)
- [18] A. Hajatzadeh et al., *An updated review on application of nanofluids in heat exchangers for saving energy*, Energy Conversion and Management, **198**, 111886 (2019)
- [19] S. Louis et al., *Application of Nanofluids in Improving the Performance of Double-Pipe Heat Exchangers—A Critical Review*, Materials, **15**, 6879 (2022)
- [20] J. Li et al., *An analysis on the compressed hydrogen storage system for the fast-filling process of hydrogen gas at the pressure of 82 MPa*, Energies, **14**, 2635 (2021)

## A Appendix - Calculation of heat transfer coefficients

Values for the heat transfer coefficients  $U$  for three differently sized concentric pipe counter-flow heat exchangers were calculated based on the CFD method and models described in Section 3.1. Typical values of the hydrogen gas mass flowrates  $\dot{m}_{H_2}$  and coolant mass flowrates  $\dot{m}_c$  were chosen. Values of  $U$  for other values of  $\dot{m}_{H_2}$  and  $\dot{m}_c$  can be found by linear interpolation. In the simulations it was assumed that the inlet temperatures of the coolants were 274 K for water and 238 K for the 50% ethylene glycol (EG) - water mixture (EG-H<sub>2</sub>O-50%) and the inlet temperature of the gas was 300 K. Since the heat transfer will depend on the density (or pressure) of the gas in the pipe, it was assumed that the exit pressure of gas from the HX (i.e., the pressure inside the tank being filled) was 100 bar (10 MPa). As shown in Section 3.2, the heat transfer does not vary significantly with pressure for exit pressure above about  $P = 30$  bar, but decreases significantly for lower values due to the low gas density. Since a composite material gas tank will typically not be emptied to more than about 20 bar, the values of  $U$  in the tables can be used for most filling calculations. In the calculations, a tube length of  $L = 10$  m was used but the heat transfer (and temperature drop) seems to vary linearly with tube length (and then coolant gas contact area  $A = 2\pi r_i \cdot L$ ) up to about  $L \approx 40$  m, as shown for water coolant in Fig. 7a) in Section 3.3. These tables may be imported as “lookup tables” in the EES software for more detailed gas bunkering calculations.

## Narrow tube heat exchanger - 10 mm radius

Coolant mass flowrate $\dot{m}_c$ [kg/s]	Gas mass flowrate $\dot{m}_{H_2}$ [kg/s]							
	0.005	0.01	0.02	0.05	0.1	0.2	0.3	0.5
0.02	260.9	325.7	383.6	435.1	452.9	452.1	438.6	410.9
0.05	331.7	417.5	506.7	623.8	689.3	724.2	724.7	700.5
0.1	459.7	643.4	855.9	1137	1307	1415	1440	1428
0.2	542	799	1116	1586	1915	2163	2253	2304
0.5	608.5	945	1411	2169	2781	3339	3606	3852
1	655.9	1049	1630	2704	3679	4667	5195	5766
2	928.2	1170	1839	3212	4620	6199	7117	8232
5	615.3	1301	3050	4004	5878	8296	9900	12043

Table 3: Heat transfer coefficients  $U$  in  $W/(m^2K)$  for various  $H_2$  gas mass flowrates  $\dot{m}_{H_2}$  and **water coolant** mass flowrates  $\dot{m}_c$  for a concentric pipe counter-flow heat exchanger of length  $L = 10$  with inner tube radius  $r_i = 10$  mm and outer tube radius  $r_o = 15$  mm.

Coolant mass flowrate $\dot{m}_c$ [kg/s]	Gas mass flowrate $\dot{m}_{H_2}$ [kg/s]							
	0.005	0.01	0.02	0.05	0.1	0.2	0.3	0.5
0.02	163.3	180.5	191.2	199	201.9	203	202.3	199.6
0.05	178.7	199.1	212.6	222.7	226.7	228.7	229.2	229
0.1	198.7	222.4	238.7	251.7	257.5	262	263.2	262.6
0.2	226.4	260	285.8	314.9	333.8	346.9	350.5	349.3
0.5	276.3	335.5	393.6	490.9	587.3	661.5	692.8	698.7
1	331.6	422.9	517.9	695.3	901.6	1070	1176	1292
2	398.8	551	787.4	1212	1528	1780	1890	1989
5	578.4	1478	1537	2109	2603	3062	3294	3536

Table 4: Heat transfer coefficients  $U$  in  $W/(m^2K)$  for a similar heat exchanger as in Table 3 using an **ethylene glycol-water 50%** mixture.

## Medium size heat exchanger - 15 mm radius

		Gas mass flowrate $\dot{m}_{H_2}$ [kg/s]								
		0.01	0.02	0.05	0.1	0.2	0.3	0.5	0.7	1
Coolant mass flowrate $\dot{m}_c$ [kg/s]	0.05	207.1	247.2	286.5	305.9	317.7	321.9	324.8	324.8	323.4
	0.1	234.7	302	399.2	463	509.2	527.7	541.9	545.4	542.7
	0.2	361.9	494.5	677.4	800	895	936	972.7	987.8	995.8
	0.5	448.1	661.1	995.5	1249	1468	1571	1674	1724	1762
	1	490.8	757.4	1233	1647	2050	2262	2486	2604	2702
	2	528.7	850.4	1492	2130	2831	3231	3692	3955	4191
	5	564.8	937.9	1766	2715	3920	4704	5699	6331	6944
	10	595.5	991.9	1910	3051	4643	5762	7293	8332	9390

Table 5: Heat transfer coefficients  $U$  in  $W/(m^2K)$  for various  $H_2$  gas mass flowrates  $\dot{m}_{H_2}$  and **water coolant** mass flowrates  $\dot{m}_c$  for a concentric pipe counter-flow heat exchanger of length  $L = 10$  with inner tube radius  $r_i = 15$  mm and outer tube radius  $r_o = 24$  mm.

		Gas mass flowrate $\dot{m}_{H_2}$ [kg/s]								
		0.01	0.02	0.05	0.1	0.2	0.3	0.5	0.7	1
Coolant mass flowrate $\dot{m}_c$ [kg/s]	0.05	110.9	119.9	126.8	129.7	131.3	132	132.4	132.6	132.6
	0.1	123.8	134.6	143	146.5	148.7	149.5	150.1	150.4	150.6
	0.2	142.5	157.8	171.1	177.1	180.7	182.1	183.3	183.8	184.2
	0.5	178.3	208	237.8	260.2	279.1	286.9	294.8	297.8	298.5
	1	215.4	262.1	327.3	389.9	452.6	483.2	512	523.5	529.4
	2	264.6	337.8	484	596.8	717.4	773.5	828.1	853.2	870.2
	5	419.2	603.2	882.5	1090	1267	1351	1436	1478	1514
	10	496.1	748.6	1192	1568	1925	2108	2302	2406	2496

Table 6: Heat transfer coefficients  $U$  in  $W/(m^2K)$  for a similar heat exchanger as in Table 5 using an **ethylene glycol-water 50%** mixture.

## Wide tube heat exchanger - 25 mm radius

		Gas mass flowrate $\dot{m}_{H_2}$ [kg/s]								
		0.01	0.02	0.05	0.1	0.2	0.3	0.5	0.7	1
Coolant mass flowrate $\dot{m}_c$ [kg/s]	0.05	92.47	110.6	129.4	139.2	145.6	148.2	150.6	151.6	152.4
	0.1	115.2	145.4	179.3	197.8	210.5	215.6	220.2	222.3	224
	0.2	136.3	182.9	244.5	283.3	312.1	324.4	335.8	341.4	345.8
	0.5	173.9	255.7	392.1	504.2	607.4	658.4	711.2	738.8	761.9
	1	201.9	314.6	521.3	708.4	897.8	999.5	1111	1172	1227
	2	216	349.3	619.6	894.9	1204	1384	1593	1714	1826
	5	226.8	378	719.3	1118	1642	1990	2443	2735	3024
	10	231.6	393.2	774.4	1255	1947	2452	3170	3669	4199

Table 7: Heat transfer coefficients  $U$  in  $W/(m^2K)$  for various  $H_2$  gas mass flowrates  $\dot{m}_{H_2}$  and **water coolant** mass flowrates  $\dot{m}_c$  for a concentric pipe counter-flow heat exchanger of length  $L = 10$  with inner tube radius  $r_i = 25$  mm and outer tube radius  $r_o = 40$  mm.

		Gas mass flowrate $\dot{m}_{H_2}$ [kg/s]								
		0.01	0.02	0.05	0.1	0.2	0.3	0.5	0.7	1
Coolant mass flowrate $\dot{m}_c$ [kg/s]	0.05	64.95	73.19	80.12	83.15	84.98	85.68	86.29	86.58	86.8
	0.1	71.86	82	90.79	94.68	97.04	97.95	98.76	99.14	99.45
	0.2	81.55	94.9	107	112.4	115.8	117	118.2	118.7	119.2
	0.5	96.64	116.7	136.5	146	152	154.4	156.6	157.6	158.4
	1	108.7	135.6	166	182.7	194.1	198.6	203	205.1	206.9
	2	121.2	157.6	204.4	234.9	267.1	273.1	285.4	291.8	296.8
	5	142.5	196.4	277.4	348.6	381.1	433.2	450.8	512.3	537.8
	10	163.9	232.7	338.5	419.7	526.4	575.6	672	706.3	764.6

Table 8: Heat transfer coefficients  $U$  in  $W/(m^2K)$  for a similar heat exchanger as in Table 7 using an **ethylene glycol-water 50%** mixture.

## Trends in the heat transfer coefficients

In order to more clearly see the systematic trends in the values of  $U$ , the data in the Tables 3-8 have been plotted in Figs. 16 - 18.

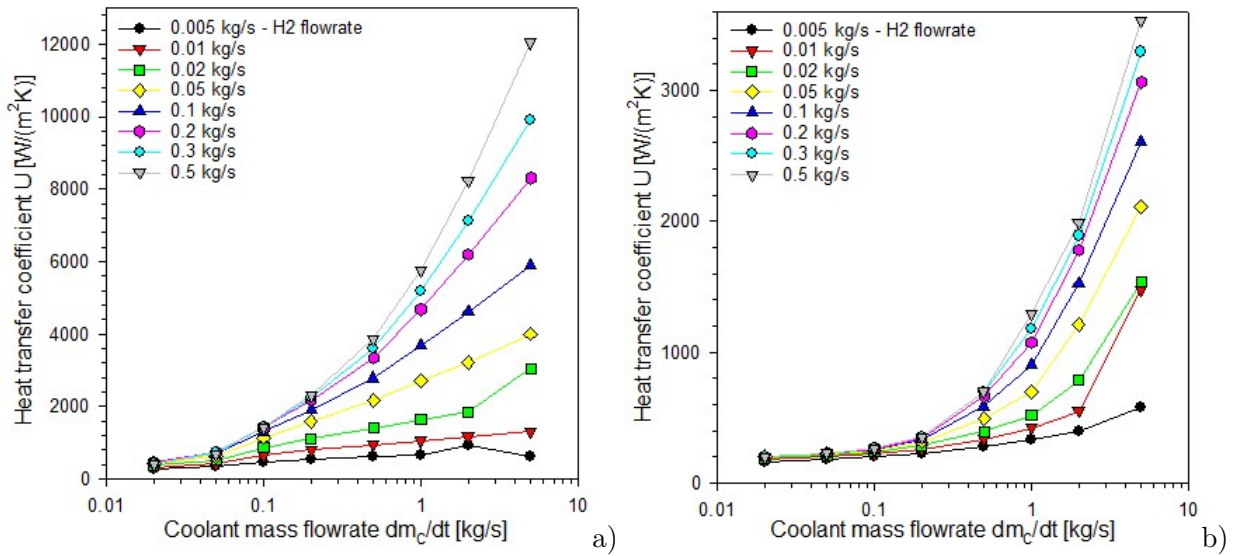


Figure 16: Heat transfer coefficients  $U$  in  $W/(m^2K)$  for a concentric pipe counter-flow heat exchanger of length  $L = 10$  with inner tube radius  $r_i = 10$  mm and outer tube radius  $r_o = 15$  mm. a) Using **water** cooling at  $T = 274$  K and b) **EG-water-50%** coolant at  $T = 238$  K.

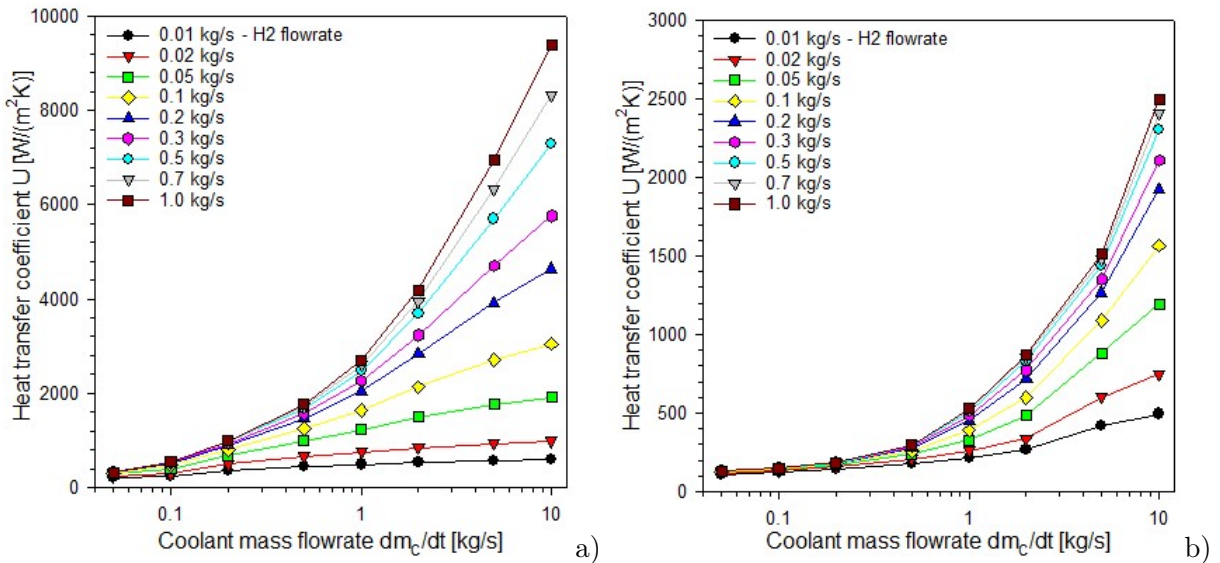


Figure 17: Heat transfer coefficients  $U$  in  $W/(m^2K)$  for a concentric pipe counter-flow heat exchanger of length  $L = 10$  with inner tube radius  $r_i = 15$  mm and outer tube radius  $r_o = 24$  mm. a) Using **water** cooling at  $T = 274$  K and b) **EG-water-50%** coolant at  $T = 238$  K.



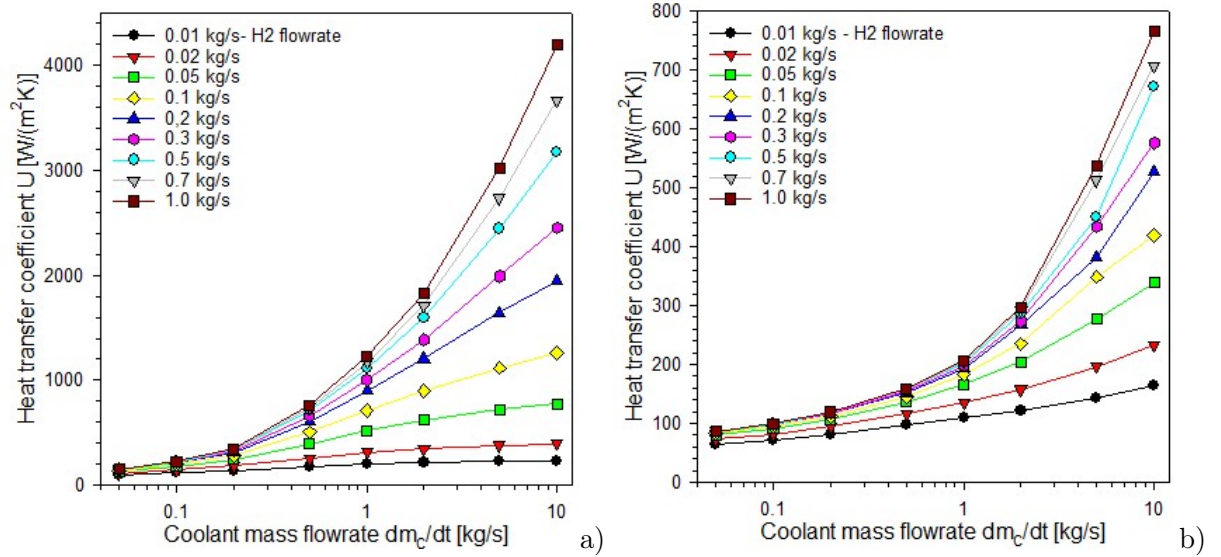


Figure 18: Heat transfer coefficients  $U$  in  $\text{W}/(\text{m}^2\text{K})$  for a concentric pipe counter-flow heat exchanger of length  $L = 10$  with inner tube radius  $r_i = 25$  mm and outer tube radius  $r_o = 40$  mm. a) Using **water** cooling at  $T = 274$  K and b) **EG-water-50%** coolant at  $T = 238$  K.

## B Appendix - EES software for temperature calculation of hydrogen tank bunkering process

Two different distributable programs (EXE-files) have been prepared as a part of the FME H2Maritime project [1] utilizing the Engineering Equation Solver (EES) software [4]. These programs simulate the transfer of hydrogen gas from a large storage tank into a number of equal size, smaller tanks in a parallel filling process. Copies of these programs can be obtained by contacting the Hydrogen Technology department at IFE.

One of the versions is a general calculation program where the cooling property of a concentric tube counter-flow heat exchanger has to be given as an input parameter  $U \cdot A_s$  ( $U$  - the heat transfer coefficient,  $A_s$  - the area of the inner tube contact surface). Two different types of coolant - water and ethylene glycol-water 50% mixtures - can be used. Figure 19 shows the input diagram of this version of the program. In the following is a short summary of how to use this program.

Input part in the middle part : The number of small tanks is given by the parameter  $N_{tank}$ , and the mass transfer rate from the large tank is given by the parameter  $\dot{m}_{H_2}$  (in  $\text{kg}/\text{s}$ ). The mass flowrate to each tank is then  $\dot{m}_{H_2}/N_{tank}$ , and the flow into each tank is cooled via a separate heat exchanger using either pure water at temperature  $T_c$  ( $>273.2$  K) or a 50:50 mixture of Ethylene Glycol (EG) and water at  $T_c$  ( $> 237.9$  K) as coolant. The coolant mass flowrate is controlled via the parameter  $\dot{m}_c$  (in  $\text{kg}/\text{s}$ ). The cooling capacity parameter  $UA_s$  (in  $\text{kW}/\text{K}$ ) has to be set by the user. Typical values are 0.1-10  $\text{kW}/\text{K}$  for water coolant and 0.05-2  $\text{kW}/\text{K}$  for EG-water operating at 238 K. The volumes of the large and smaller tanks are defined by parameters  $V_{tank}$  (in  $\text{m}^3$ ), and the heat capacities of the tanks walls are  $C_w$  [in  $\text{kJ}/(\text{m}^2\text{K})$ ]. For the smaller tanks, their radius  $r$  [m] is needed for the calculation of the total surface area. Initial temperature and pressure of tanks are set by parameters  $T_1$ ,  $P_1$  and  $T_2$ ,  $P_2$  (in K and MPa). The filling time in seconds is set by  $Time$ , and the program will give a warning if pressure in the smaller tanks reaches pressure in the main tank. Simulation is

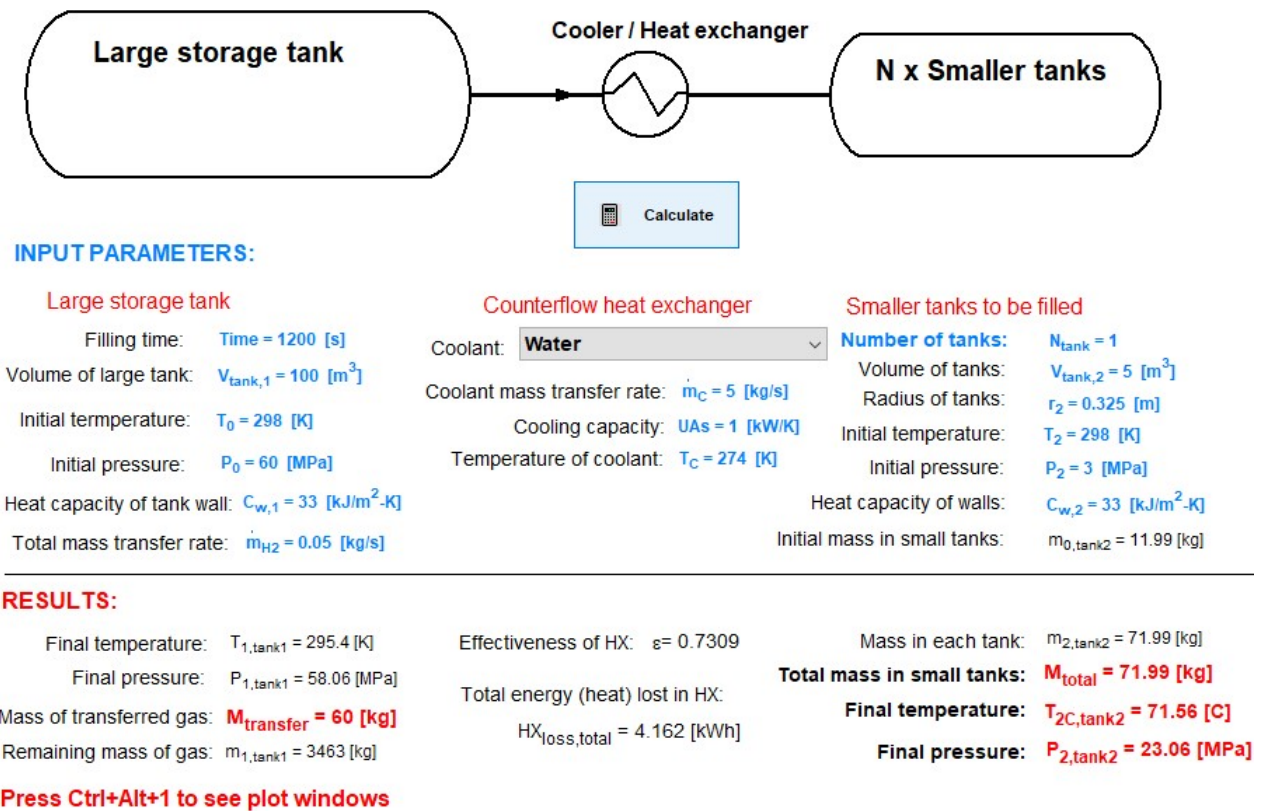
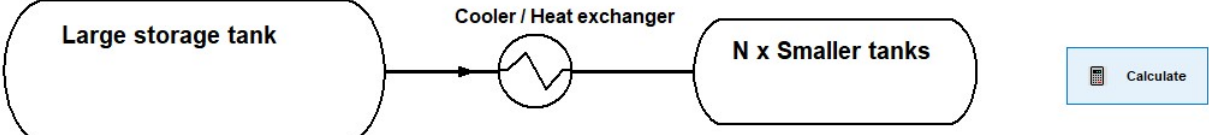


Figure 19: User input diagram window for the general purpose bunkering program.

started by pressing the **Calculate** button.

The results part in the lower part of the diagram window lists the final temperatures and pressures in the tanks along with total amount of gas that has been transferred and final masses of gas in large and small tanks. Also, the effectiveness  $\epsilon$  of the heat exchanger under current operation conditions will be given. More details from the calculations can be found by choosing **Solution** under the Windows Tab. The results are presented graphically in the four **Plot Windows**.

In the second program, parameters for three differently sized heat exchangers are included in the model; one smaller based on i) 20 mm inner tube diameter (hydrogen tube); one intermediate size with ii) 30 mm diameter inner tube; and one larger size with iii) 50 mm diameter inner tube. The separation between inner and outer tubes used for coolant (thickness of the “annulus”) are i) 5 mm, ii) 9 mm, and iii) 15 mm. The length of the heat exchangers are fixed at 10 m, and effects of bending or curved shapes are ignored in the calculations. By choosing one of these options the correct value for the cooling capacity parameter  $UAs$ , is taken from a “Lookup table” inside the program. These values were calculated from CFD calculations using COMSOL Multiphysics software as described in the main text, and their values are given in Appendix A. The temperature of the coolant is set to 1 °C for water or –35 °C for the 50:50 EG-water mixture. EG-water cooling can be chosen by the checkbox near the center of the diagram window; else water cooling is assumed. The rest of the user input and results output are the same as in the first version.



**INPUT PARAMETERS:**

**Large storage tank**

Filling time:  $\text{Time} = 1500$  [s]  
 Volume of large tank:  $V_{\text{tank},1} = 100$  [m<sup>3</sup>]  
 Initial temperature:  $T_1 = 298$  [K]  
 Initial pressure:  $P_1 = 60$  [MPa]  
 Heat capacity of tank wall:  $C_{w,1} = 33$  [kJ/m<sup>2</sup>·K]  
 Total mass transfer rate:  $\dot{m}_{\text{H}_2} = 0.05$  [kg/s]

**Counterflow heat exchanger**

Use Ethylene Glycol-Water-50%  
 Coolant flowrate for small tank:  $\dot{m}_c = 2.5$  [kg/s]

Choose One Option:

Large size heat exchanger (50 mm inner tube diameter)  
 Medium size heat exchanger (30 mm inner tube diameter)  
 Small size heat exchanger (20 mm inner tube diameter)

**Smaller tanks to be filled**

**Number of tanks:**  $N_{\text{tank}} = 1$   
 Volume of tanks:  $V_{\text{tank},2} = 5$  [m<sup>3</sup>]  
 Radius of tanks:  $r_2 = 0.325$  [m]  
 Initial temperature:  $T_2 = 298$  [K]  
 Initial pressure:  $P_2 = 10$  [MPa]  
 Heat capacity of walls:  $C_{w,2} = 33$  [kJ/m<sup>2</sup>·K]  
 Initial mass in small tanks:  $m_{0,\text{tank}2} = 38.37$  [kg]

**RESULTS:**

Final temperature:  $T_{1,\text{tank}1} = 294.8$  [K]  
 Final pressure:  $P_{1,\text{tank}1} = 57.58$  [MPa]  
 Mass of transferred gas:  $M_{\text{transfer}} = 75$  [kg]  
 Remaining mass of gas:  $m_{1,\text{tank}1} = 3448$  [kg]

Effectiveness of HX:  $\varepsilon = 0.7251$   
 Heat transfer coefficient:  $U = 0.6362$  [kW/m<sup>2</sup>-K]  
 Total energy (heat) lost in HX:  
 $\text{HX}_{\text{loss,total}} = 5.089$  [kWh]

Mass in each tank:  $m_{2,\text{tank}2} = 113.4$  [kg]  
**Total mass in small tanks:  $M_{\text{total}} = 113.4$  [kg]**  
**Final temperature:  $T_{2C,\text{tank}2} = 72.86$  [C]**  
**Final pressure:  $P_{2,\text{tank}2} = 39.44$  [MPa]**

**Press Ctrl+Alt+1 to see plot windows**

Figure 20: User input window for the program with three differently sized heat exchanger options for cooling.